

Dalton Transactions

Accepted Manuscript



This article can be cited before page numbers have been issued, to do this please use: L. M. Mesquita, P. Mateus, R. D. V. Fernandes, O. Iranzo, V. André, F. Tiago de Oliveira, C. Platas-Iglesias and R. Delgado, *Dalton Trans.*, 2017, DOI: 10.1039/C7DT01724C.



This is an Accepted Manuscript, which has been through the Royal Society of Chemistry peer review process and has been accepted for publication.

Accepted Manuscripts are published online shortly after acceptance, before technical editing, formatting and proof reading. Using this free service, authors can make their results available to the community, in citable form, before we publish the edited article. We will replace this Accepted Manuscript with the edited and formatted Advance Article as soon as it is available.

You can find more information about Accepted Manuscripts in the [author guidelines](#).

Please note that technical editing may introduce minor changes to the text and/or graphics, which may alter content. The journal's standard [Terms & Conditions](#) and the ethical guidelines, outlined in our [author and reviewer resource centre](#), still apply. In no event shall the Royal Society of Chemistry be held responsible for any errors or omissions in this Accepted Manuscript or any consequences arising from the use of any information it contains.

Recognition of Phosphopeptides by a Dinuclear Copper(II) Macrocyclic Complex in Water:Methanol 50:50 v/v Solution

Lígia M. Mesquita,^a Pedro Mateus,^a Rui D. V. Fernandes,^a Olga Iranzo,^b Vânia André,^c Filipe Tiago de Oliveira,^d Carlos Platas-Iglesias,^e Rita Delgado*^a

^a Instituto de Tecnologia Química e Biológica António Xavier, Universidade Nova de Lisboa, Av. da República, 2780–157 Oeiras, Portugal.

^b Aix Marseille Univ., CNRS, Centrale Marseille, iSm2, Marseille, France

^c Centro de Química Estrutural, Instituto Superior Técnico, Universidade de Lisboa, Av. Rovisco Pais, 1049–001 Lisboa, Portugal.

^d Laboratório de Instrumentação, Engenharia Biomédica e Física da Radiação (LIBPhys-UNL), Departamento de Física, Faculdade de Ciências e Tecnologia da Universidade Nova de Lisboa, Monte de Caparica, 2892–516 Caparica, Portugal.

^e Centro de Investigaciones Científicas Avanzadas (CICA) and Departamento de Química Fundamental, Facultad de Ciencias, Universidad da Coruña, Campus da Zapateira-Rúa da Fraga 10, 15008 A Coruña, Spain.

Electronic supplementary information (ESI) available: Tables of overall protonation constants of L and of the studied substrates, of overall stability constants of copper(II) with the studied substrates, and overall association constants between the copper(II) complexes of L with the substrates. Figures of species distribution of L, H₂pST3 and of cascade species with peptides. Figure of the EPR spectra of the copper(II) complexes at different pH values. Figures of 1D, 2D NMR and ESI mass spectra of the L compound, of the phosphopeptides, and of some intermediate compounds: 2,4-bis(bromomethyl)-1,3,5-triethylbenzene and (2,4,6-triethyl-1,3-phenylene)dimethanamine. DFT results.

ABSTRACT

A new triethylbenzene-derived tetraazamacrocycle containing pyridyl spacers, L, was prepared and its dinuclear copper(II) complex was used as receptor for the recognition of phosphorylated peptides in aqueous solution. A detailed study of the acid-base behaviour of L and its copper(II) complexation properties as well as of the cascade species with phosphorylated anions including two peptidic substrates was carried out in H₂O/MeOH (50:50 v/v) solution using different techniques, such as potentiometry, X-band EPR and DFT calculations. The association constants of the dinuclear receptor with the phosphorylated peptides and other anionic species revealed a clear preference towards phenylic phosphorylated substrates, with values ranging 3.96–5.35 log units. Single-crystal X-ray diffraction determination of the dicopper(II) complex of L showed the copper centres at a distance of 5.812(1) Å from one another, with the phosphate group of the PhPO₄²⁻ substrate well accommodated between them. X-band EPR studies indicated a similar structure for this cascade complex and for the other cascade complexes with the phosphorylated anions studied. DFT studies of the [Cu₂L(μ-OH)]³⁺ complex revealed a different conformation of the ligand that brings the two copper centres at a very short distance of 3.94 Å aided by the presence of a bridging hydroxide anion that provides a Cu...O...Cu angle of 167.3°. This complex is EPR silent, in line with the singlet ground state obtained using CASSCF(2,2) calculations and DFT calculations with the broken-symmetry approach. This species coexists in solution with a complex in a different conformation, and having a Cu...Cu distance of 6.63 Å, in lower percentage.

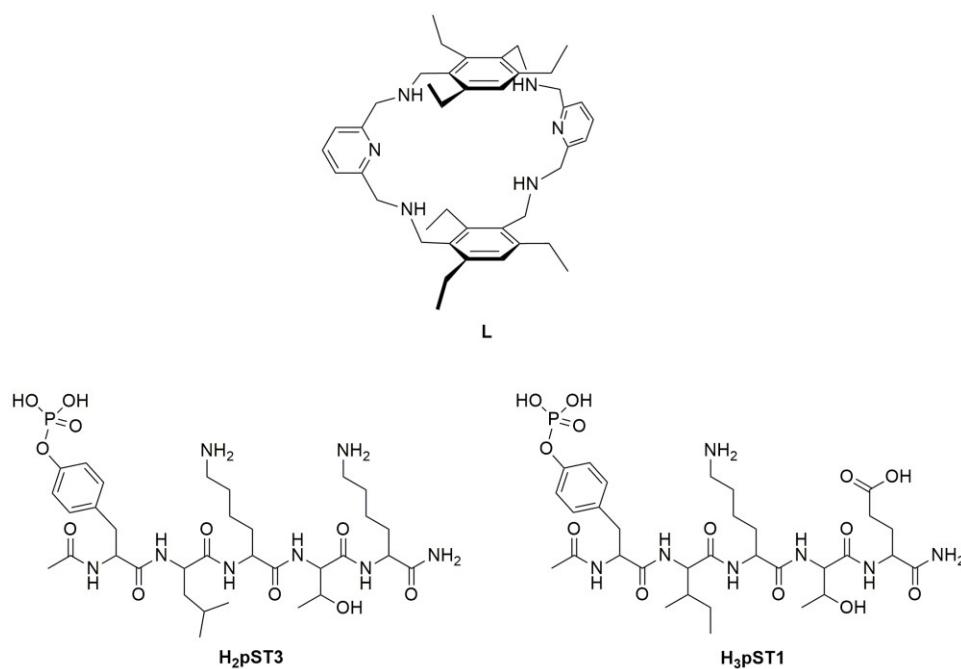
INTRODUCTION

Protein phosphorylation is a key event in the signalling pathways that control many cell functions including metabolism, transcription, cell cycle progression, apoptosis, and differentiation.¹ Aberrant protein phosphorylation/dephosphorylation is observed in several human pathologies, including inflammatory, neurodegenerative and autoimmune diseases,² and cancer.³ Phosphorylation of tyrosine, threonine and serine residues on protein surfaces serves as a switch either by creating binding sites for the establishment of protein-protein interactions or by promoting conformational changes that activate enzymatic activity.⁴ Therefore, compounds able to bind phosphopeptides/phosphoproteins can potentially be used as inhibitors of a particular deregulated signalling pathway or as analytical tools for investigating phosphorylation-based cell signaling.⁵

However, the recognition of phosphorylated peptides or proteins in the presence of other bio-relevant anionic molecules is not straightforward. In fact, the binding of phosphorylated substrates with high affinity and selectivity in aqueous media still remains a great research challenge.⁶ Notwithstanding attempts have been made in order to develop suitable receptors for the recognition of phosphopeptides/phosphoproteins. Among them, dinuclear metal complexes of ligands derived from dipicolylamine or cyclen have been used for this purpose.⁷ Although the use of dinuclear metal complexes for the binding of anionic substrates in aqueous medium is a proven strategy, achieving selectivity through the formation of cascade species involves the location of the metal centres at a given relatively rigid fixed distance,⁸ a requirement difficult to accomplish with non-cyclic ligands.

In this work, the dinuclear complexes of a ditopic hexaamine macrocycle are evaluated as a possible alternative to non-cyclic ligands. Macrocyclic complexes were already used as receptors for the uptake of phosphorylated substrates.⁹ However, to the best of our knowledge, studies reporting binding of phosphorylated peptides to dinuclear complexes of macrocyclic ligands are scarce.¹⁰ In these receptors, each metal centre is designed with one or two coordination sites occupied by water molecules or weakly coordinated counterions easily replaced by the envisaged substrate, while the distance between the two metal centres is modulated by rigid spacers.⁸

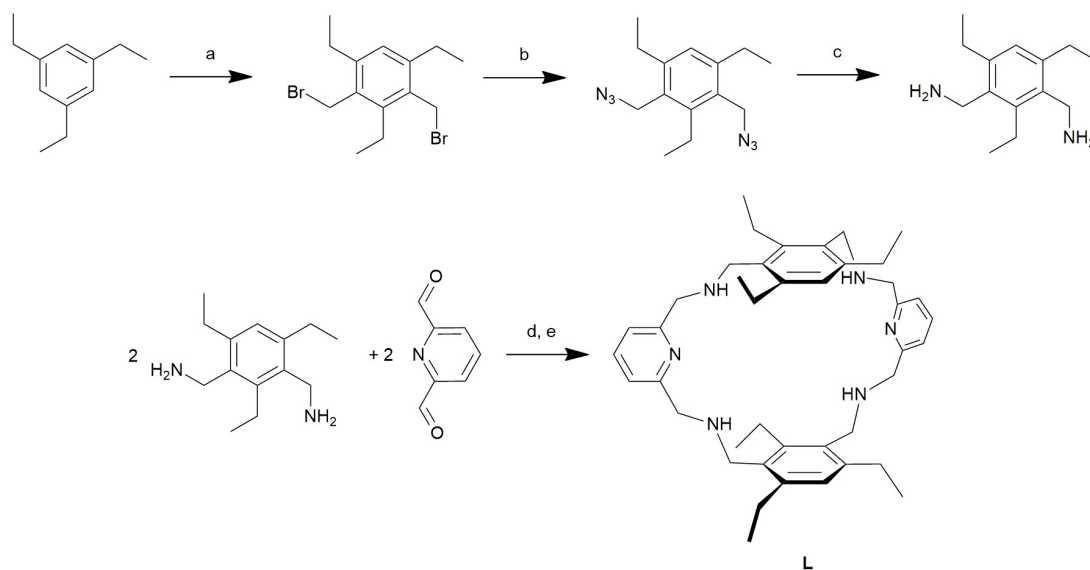
In the present study a new triethylbenzene-derived tetraazamacrocycle containing pyridyl spacers (L, Scheme 1) is described and its dinuclear copper(II) complex evaluated as a receptor for phosphorylated peptides. The compound was prepared under the expectation that while the pyridyl heads would function as metal binding sites, the triethylbenzene groups might be engaged in π - π interactions with the benzene group of phosphotyrosine. Peptides H₃pST1 and H₂pST3 (Scheme 1) were selected as models of the phosphorylated sequences of signal transducer and activator of transcription proteins STAT1¹¹ and STAT3.¹² These sequences are involved in the homo and heterodimerization of the latter proteins, a crucial event for nucleus translocation and subsequent up-regulation of several genes involved in cell progression, differentiation, and survival.¹³



Scheme 1 Ligand L and peptides studied in this work.

RESULTS AND DISCUSSION

Synthesis of compound L. The synthesis of L started with the preparation of 2,4-bis(bromomethyl)-1,3,5-triethylbenzene from commercially available 1,3,5-triethylbenzene (Scheme 2, steps a to c). Although this compound has been described previously,¹⁴ the product was not isolated and instead used as a mixture of di- and tribromomethylated compounds. Herein, by using 3 equiv. of paraformaldehyde and HBr relative to 1,3,5-triethylbenzene, and a precise control of the reaction temperature at 80 °C,¹⁵ the desired compound was obtained in 77% yield. The dibromide was then converted to the diazide, followed by reduction with Ph₃P in THF/H₂O to afford the 2,4-bis(aminomethyl)-1,3,5-triethylbenzene, using a procedure similar to that described for the preparation of 2,4,6-tris(aminomethyl)-1,3,5-triethylbenzene.¹⁶ Compound L was then obtained in good yield by reaction between 2,4-bis(aminomethyl)-1,3,5-triethylbenzene and 2,6-pyridinedicarbaldehyde in 2:2 ratio in MeCN, followed by addition of sodium borohydride for the reduction of imine groups to the corresponding amines (Scheme 2, steps d and e). This compound is the macrocyclic version of a cryptand reported by us.¹⁷



Scheme 2 Synthetic procedure for the preparation of L. a) Zn, 3 equiv. (HCOH)_n, 33% HBr in AcOH, 80 °C, $\eta = 77\%$; b) NaN₃, DMF, r.t., $\eta = 94\%$; c) Ph₃P, THF:H₂O (10:1), r.t., $\eta = 73\%$; d) MeOH, r.t., $\eta = 77\%$; e) NaBH₄, MeOH, reflux, $\eta = 92\%$.

The H₂pST3 peptide (Scheme 1) was obtained commercially and already used by us,¹⁰ and the H₃pST1 peptide was synthesized by using Fmoc chemistry,¹⁸ and was purified by preparative reversed-phase HPLC.

Acid-base behaviour of L and H₃pST1 and H₂pST3 peptides, and copper(II) complexation studies

The protonation constants of L and its stability constants with Cu²⁺ were determined at ionic strength 0.10 M in KNO₃ and 298.2 K in H₂O/MeOH (50:50 v/v). The studies were performed in a mixed solvent system due to the precipitation of the ligand at pH 6.0 in pure water, preventing the determination of the protonation constants in this medium. Furthermore, the copper(II) complex also precipitates at pH > 7.0 at the concentrations required for potentiometric titrations. The corresponding stepwise constants are collected in Table 1, and the overall constants are presented in Table S1 in the ESI. The species distribution diagram for the protonation of L is shown in Fig. S1 in the ESI.

The four protonation constants determined for L correspond to the successive protonation of the secondary amines. The pyridyl nitrogen atoms are not protonated in the working pH range (3.5–10.5). The results agree well with those previously reported for the related macrobicyclic compound.^{17,19}

The copper(II) complexation studies of L revealed its very high tendency to form dinuclear complexes. Indeed, even at 1:1 Cu²⁺:L ratio (Fig. 1a), the dinuclear species start to form at pH 3.5 being the predominant species at pH > 5.8. The stepwise stability constant of the dinuclear complex

$[\text{Cu}_2\text{L}]^{4+}$ (coordinated H_2O molecules are omitted for simplicity), obtained by reaction of Cu^{2+} with $[\text{CuL}]^{2+}$, is lower than the stability constant of the mononuclear complex by 4.18 log units due to the charge repulsion between the two closely located metal ions, besides the statistical factor. Nonetheless, at 2:1 $\text{Cu}^{2+}:\text{L}$ ratio (Fig. 1b), the dinuclear species predominate above pH 4.5, and exist mainly in the form of the monohydroxo complex, $[\text{Cu}_2\text{L}(\text{OH})]^{3+}$. This hydroxo complex starts to form at a very unusual low pH ($\text{p}K_a = 4.42$), indicating that the hydroxide anion bridges the two copper centres that thus must be located at short distance from one another (see discussion below). The value of the association constant of OH^- with the $[\text{Cu}_2\text{L}]^{4+}$ receptor takes the high value of 9.43 log units (see Table 1). Similar low $\text{p}K_a$ values for the hydrolysis of a coordinated water molecule were found in a few dicopper(II) complexes of cryptands.²⁰ However, the $\text{p}K_a$ value found in this work is, to the best of our knowledge, the lowest value found for a dinuclear copper(II) complex of a macrocycle. In fact, the deprotonation of one coordinated water molecule lowers the positive charge in the pocket formed between the copper(II) centres at short distance, contributing to minimize the electrostatic repulsions. Two other μ -hydroxo dicopper(II) complexes of macrocyclic ligands were found to have very short $\text{Cu}\cdots\text{Cu}$ distances in their X-ray structures, but the $\text{p}K_a$ values of the water deprotonation were not determined.²¹

Table 1 Stepwise protonation constants (K_i^{H}) of L and stepwise stability constants ($K_{\text{Cu}_m\text{H}_h\text{L}}$) of its copper(II) complexes in $\text{H}_2\text{O}/\text{MeOH}$ (50:50 v/v).^a

Equilibrium reaction	$\log K_i^{\text{H}b}$	Equilibrium reaction	$\log K_{\text{Cu}_m\text{H}_h\text{L}}^b$
$\text{L} + \text{H}^+ \rightleftharpoons \text{HL}^+$	8.36(1)	$[\text{CuHL}]^{3+} + \text{H}^+ \rightleftharpoons [\text{CuH}_2\text{L}]^{4+}$	5.85(2)
$\text{HL}^+ + \text{H}^+ \rightleftharpoons \text{H}_2\text{L}^{2+}$	7.52(1)	$[\text{CuL}]^{2+} + \text{H}^+ \rightleftharpoons [\text{CuHL}]^{3+}$	7.10(2)
$\text{H}_2\text{L}^{2+} + \text{H}^+ \rightleftharpoons \text{H}_3\text{L}^{3+}$	6.51(1)	$\text{Cu}^{2+} + \text{L} \rightleftharpoons [\text{CuL}]^{2+}$	11.24(3)
$\text{H}_3\text{L}^{3+} + \text{H}^+ \rightleftharpoons \text{H}_4\text{L}^{4+}$	5.79(1)	$[\text{CuL}(\text{OH})]^+ + \text{H}^+ \rightleftharpoons [\text{CuL}]^{2+}$	8.38(2)
–	–	$[\text{CuL}]^{2+} + \text{Cu}^{2+} \rightleftharpoons [\text{Cu}_2\text{L}]^{4+}$	7.06(3)
–	–	$[\text{Cu}_2\text{L}(\text{OH})]^{3+} + \text{H}^+ \rightleftharpoons [\text{Cu}_2\text{L}]^{4+}$	4.42(1)
–	–	$[\text{Cu}_2\text{L}]^{4+} + \text{OH}^- \rightleftharpoons [\text{Cu}_2\text{L}(\text{OH})]^{3+}$	9.43(3)

^a $T = 298.2 \pm 0.1$ K; $I = 0.10 \pm 0.01$ M in KNO_3 . ^b Values in parenthesis are standard deviations in the last significant figures.

Precipitation of the $[\text{Cu}_2\text{L}(\text{OH})]^{3+}$ complex (or $[\text{Cu}_2\text{L}(\text{OH})_2]^{2+}$ starting to be formed) occurred above pH 8.00, which prevented further characterization of the system in solution, but at least it was possible

to infer that one other possible coordinated water molecule only deprotonates at higher and more usual pH, and so this hydroxide anion is likely not bridging the two copper centres.

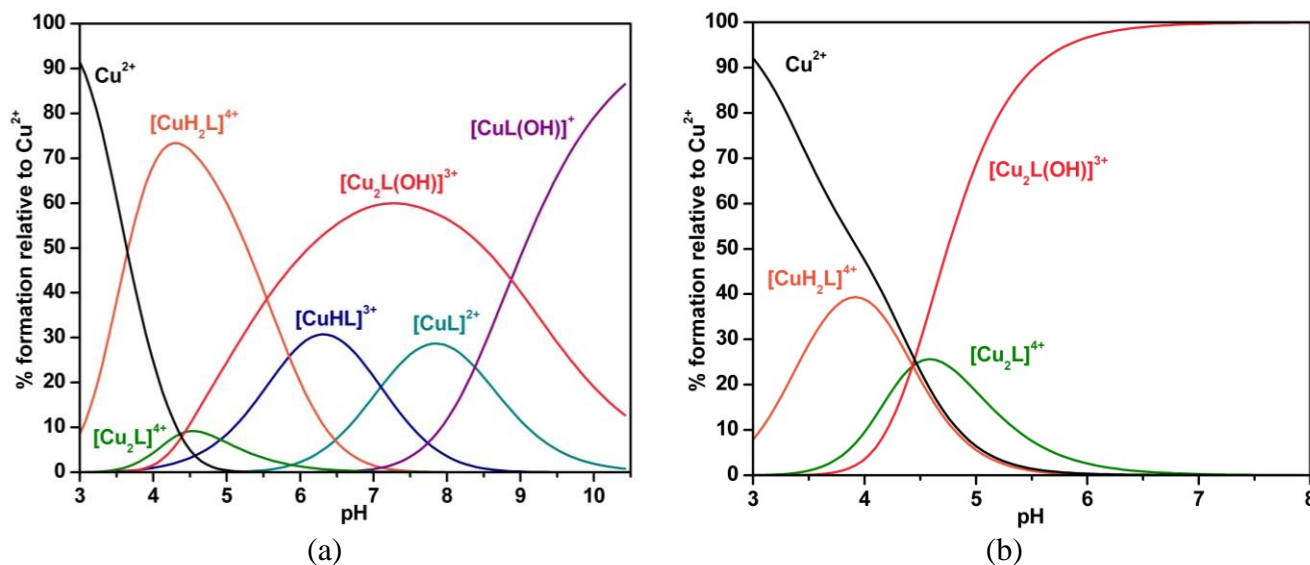


Fig. 1 Species distribution diagrams calculated for the complexes of Cu^{2+} with L. (a) Cu:L 1:1 ratio, $C_{\text{Cu}} = C_{\text{L}} = 2.0 \times 10^{-3}$ M; and (b) Cu:L 2:1 ratio, $C_{\text{Cu}} = 2C_{\text{L}} = 2.0 \times 10^{-3}$ M.

The protonation constants for the studied anions were also determined in the same experimental conditions, including $\text{H}_2\text{pST3}$,¹⁰ see Table S2 and Fig. S2 in the ESI. For the $\text{H}_3\text{pST1}$ peptide the first K_1^{H} value corresponds to the protonation of the lysine amine group in agreement with the value obtained for $\text{H}_2\text{pST3}$. The second constant, K_2^{H} , is mainly attributed to the protonation of the phosphonate group of the phosphotyrosine (pY), agreeing well with the values obtained for the protonation of PhPO_4^{2-} and of the pY of $\text{H}_2\text{pST3}$. As a consequence, the HpST1^{2-} species, which contains completely ionized anionic groups and a protonated lysine, dominates a very large pH range (Fig. 2). In this peptide the K_3^{H} constant is mainly attributed to the protonation of the glutamate residue, in agreement with the value obtained for acetate ($\log K_1^{\text{H}} = 5.24$, see Table S2 in the ESI). These considerations can be visualized by the speciation diagrams shown in Figs. 2 and S2. In all cases, due to their high basicity, the amide centres remain protonated in solution within the pH range accessible by potentiometry, and so it was impossible to determine their protonation constants.

The copper(II) complexation properties of the anions were also studied in the same conditions (Table S3 in ESI). The peptidic substrates exhibit low affinity for copper(II), as expected of peptides with blocked N-termini containing only weakly coordinating side chains.²² This means that the side chains of the peptide, the pY in particular, do not participate in metal ion coordination. Due to the low

affinity of H₂pST1 for copper(II), determination of stability constants required using an excess of peptide relative to the copper(II) ion and to perform back-titrations.

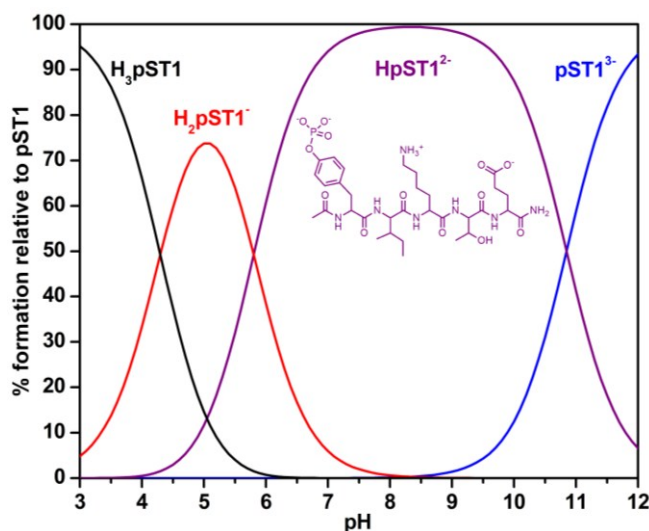


Fig. 2 Species distribution diagrams for the protonation of H₃pST1. $C_{\text{peptide}} = 1.0 \times 10^{-3}$ M.

Cascade species formed by the copper(II) complexes of L with phosphorylated substrates.

The very high association constant of the receptor to OH⁻, prompted us to study the association of the dinuclear copper(II) complexes of L as receptor to *p*-cresol in order to test its binding ability towards phenolic substrates. However, no association was detected within the working pH range. The receptor was then used for the binding of phosphorylated anions. The corresponding association constants were determined by potentiometry at the experimental conditions used before, and the results are collected in Table 2 (see also Table S4 in the ESI). Experiments with one non-phosphorylated peptide derivative of H₂pST3, HST3,^{10c} were also carried out. However, precipitation during the titration prevented us from determining its stability constant with Cu²⁺ ion.

The receptor was found to form stable 1:1 associations with H_nPO₄⁽³⁻ⁿ⁾⁻ and with H_nPhPO₄⁽²⁻ⁿ⁾⁻, interacting with the anions in the form of [Cu₂L]⁴⁺ as well as [Cu₂L(OH)]³⁺ (see Tables 2 and Table S4 in ESI). The high affinity of the substrates for the hydroxocomplex [Cu₂L(OH)]³⁺ suggests that the OH⁻ anion co-operates with the binding event. In fact, the hydroxide anion contributes to deprotonate the phosphonate anions at a pH value lower than expected. Indeed, the pK_a of H₂PO₄⁻ is 7.51 (H₂PO₄⁻ ⇌ HPO₄²⁻ + H⁺ pK_a = 7.51) whereas when the same anion is coordinated to both copper centres forming the cascade species its pK_a is much lower of about 4 ([Cu₂L(H₂PO₄)]³⁺ ⇌ [Cu₂L(HPO₄)]²⁺ + H⁺ pK_a = 4.00). Furthermore, the formation of the [Cu₂L(OH)]³⁺ species likely pre-organises the complex by

bringing the two metal ions at a short distance, so that coordination of bridging phosphorylated anions is favoured (see X-ray analysis below). Also noteworthy is the fact that PhPO_4^{2-} is bound 0.64 log units stronger than HPO_4^{2-} , in spite of its lower basicity, which suggests π - π interactions established between the triethylbenzene units of the receptor and the phenyl group of the substrate may contribute to the overall affinity.

The high affinity of the receptor towards PhPO_4^{2-} encouraged us to study the interaction of the receptor with phosphorylated peptides, see Table 2. Indeed, high values of association constants were determined for the binding of the receptor with the protonated forms of the phosphorylated peptides, ranging 3.96–5.35 log units. Moreover, only species of 1:1 receptor:substrate stoichiometry were found for all the cases, see Table 2 and the species distribution diagram in Fig. S3 in the ESI. The association constants increase as the overall charge of the substrates decreases, as would be expected based on electrostatic arguments. Accordingly, as the $\text{H}_3\text{pST1}$ peptide has a positive charge one unit lower than that of $\text{H}_2\text{pST3}$ at any given pH value, the receptor shows a preference for the former peptide over $\text{H}_2\text{pST3}$ due to decreased electrostatic repulsions.

Table 2 Stepwise association constants ($K_{\text{Cu}_2(\text{H}_h\text{L})\text{S}}$) for the indicated equilibria in $\text{H}_2\text{O}/\text{MeOH}$ (50:50 v/v).^a

Equilibrium reaction	$\log K_{\text{Cu}_2(\text{H}_h\text{L})\text{S}}^b$
$[\text{Cu}_2\text{L}]^{4+} + \text{H}_2\text{PO}_4^- \rightleftharpoons [\text{Cu}_2\text{L}(\text{H}_2\text{PO}_4)]^{3+}$	4.09(3)
$[\text{Cu}_2\text{L}(\text{OH})]^{3+} + \text{H}_2\text{PO}_4^- \rightleftharpoons [\text{Cu}_2\text{L}(\text{HPO}_4)]^{2+}$	4.51(2)
$[\text{Cu}_2\text{L}(\text{OH})]^{3+} + \text{H}(\text{PhPO}_4)^- \rightleftharpoons [\text{Cu}_2\text{L}(\text{PhPO}_4)]^{2+}$	5.16(1)
$[\text{Cu}_2\text{L}]^{4+} + \text{H}_3\text{pST3}^+ \rightleftharpoons [\text{Cu}_2\text{L}(\text{H}_3\text{pST3})]^{5+}$	3.96(6)
$[\text{Cu}_2\text{L}(\text{OH})]^{3+} + \text{H}_3\text{pST3}^+ \rightleftharpoons [\text{Cu}_2\text{L}(\text{H}_2\text{pST3})]^{4+}$	4.87(1)
$[\text{Cu}_2\text{L}]^{4+} + \text{H}_3\text{pST1} \rightleftharpoons [\text{Cu}_2\text{L}(\text{H}_3\text{pST1})]^{4+}$	4.62(3)
$[\text{Cu}_2\text{L}(\text{OH})]^{3+} + \text{H}_3\text{pST1} \rightleftharpoons [\text{Cu}_2\text{L}(\text{H}_2\text{pST1})]^{3+}$	5.05(1)
$[\text{Cu}_2\text{L}(\text{OH})]^{3+} + \text{H}_2\text{pST1}^- \rightleftharpoons [\text{Cu}_2\text{L}(\text{HpST1})]^{2+}$	5.35(1)

^a $T = (298.2 \pm 0.1)$ K; $I = (0.10 \pm 0.01)$ M in KNO_3 . ^b Values in parenthesis are standard deviations in the last significant figures.

In addition, it was found that the association constant values for the $[\text{Cu}_2\text{L}(\text{OH})]^{3+} + \text{H}_2\text{pST1}^- \rightleftharpoons [\text{Cu}_2\text{L}(\text{HpST1})]^{2+}$ and $[\text{Cu}_2\text{L}(\text{OH})]^{3+} + \text{H}_3\text{pST3}^+ \rightleftharpoons [\text{Cu}_2\text{L}(\text{H}_2\text{pST3})]^{4+}$ equilibria are of the same magnitude of that obtained for the $[\text{Cu}_2\text{L}(\text{OH})]^{3+} + \text{H}(\text{PhPO}_4)^- \rightleftharpoons [\text{Cu}_2\text{L}(\text{PhPO}_4)]^{2+}$ equilibrium, which suggests that both peptides are bound to the receptor through the phosphonate group of the phosphotyrosine (pY residue).

In order to evaluate the possible impact of the direct binding of the studied anions with protonated species of the ligand (H_nL^{n+}), the association constant of $PhPO_4^{2-}$ with the free ligand was determined. It was verified that the obtained value of 2.20 in log units for the association constant corresponding to the equilibrium $H_4L^{4+} + HPhPO_4^- \rightleftharpoons H_5LPhPO_4^{3+}$ is very low. The percentage of this species in presence of the copper(II) is $\sim 10\%$ at pH 3.0 and negligible at pH 4.0 (see the species distribution shown in Fig. S3 in the ESI). As the association constants of (H_nL^{n+}) with the other studied phosphorylated anions are expected to be similar or even lower than the one determined for $PhPO_4^{2-}$ anion, it is possible to conclude that the association of the free ligand with the anion does not affect at the determinations of the associations of the studied anions with the dicopper complex receptor.

Single Crystal X-Ray Diffraction Studies. The molecular structure of $[Cu_2L(\mu-PhPO_4)][Cu_2L(\mu-PhPO_4)(NO_3)]3NO_3 \cdot 24H_2O$ is shown in Fig. 3 along with the relevant atomic notation adopted. Selected distances and angles are given in Table 3.

The asymmetric unit contains two independent dinuclear copper(II) complex cations: $[Cu_2L(\mu-PhPO_4)]^{2+}$ (A) and $[Cu_2L(\mu-PhPO_4)(NO_3)]^+$ (B) (see Fig. 3a). In complex cation A each copper centre exhibits a distorted square planar geometry composed of three nitrogen donors from the 2,6-bis(aminomethyl)pyridine moieties of the macrocycle and one oxygen atom of the bound substrate. The phosphate group of the $PhPO_4^{2-}$ substrate is well accommodated between the two copper centres, placing them at a distance of 5.812(1) Å from one another. It bridges the two Cu centres in a *syn-anti* mode which results in a non-collinearity of the two N8A–Cu1A–O1A and N26A–Cu2A–O3A axes and an angle of 29.1(2)° between both CuN_3O coordination planes. The dianion is strongly bound to the metal centres, as evidenced by the short Cu–O distances (Cu1A–O1A and Cu2A–O3A distances of 1.872(4) and 1.862(6) Å, respectively).

The complex cation B presents very similar bond lengths and angles (see Table 3) and mainly differs in the coordination of the Cu2 atom, which is pentacoordinate. In this case the basal plane is defined by the three nitrogen donors from the macrocycle and one oxygen atom of the bound substrate while an oxygen atom of one nitrate anion occupies the apical position. The trigonal distortion calculated using the index structural parameter τ ($\tau = 0$ for a perfect square-pyramidal geometry and $\tau = 1$ for an ideal trigonal-bipyramidal geometry)²³ assumes a value of 0.19 which is consistent with a distorted square pyramidal coordination sphere. As in complex cation A, the phosphate group of $PhPO_4^{2-}$ bridges the two copper centres in a *syn-anti* mode which results in a Cu...Cu distance of 5.811(1) Å.

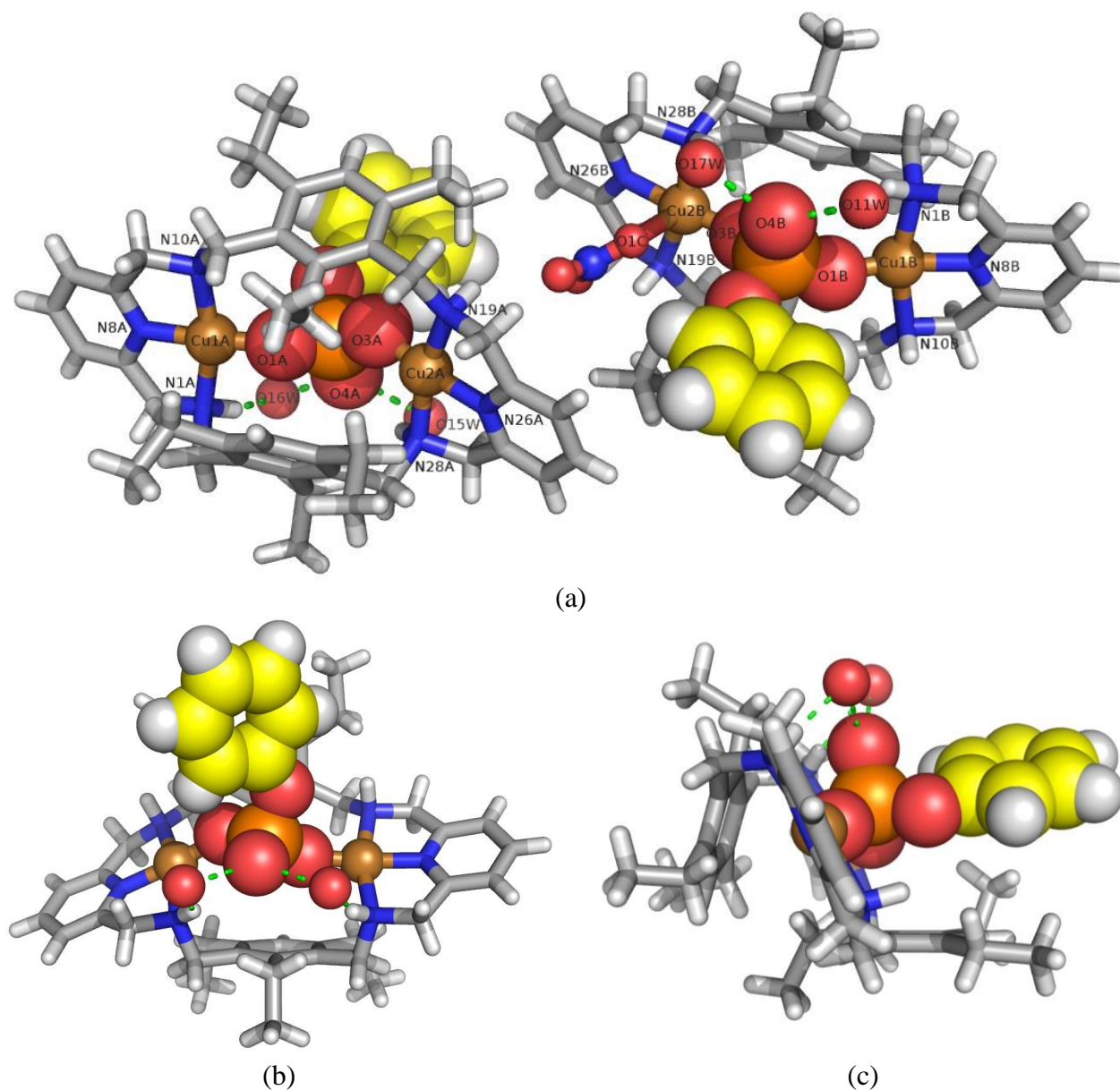


Fig. 3 (a) Molecular structure of $[\text{Cu}_2\text{L}(\mu\text{-PhPO}_4)]^{2+}$ and $[\text{Cu}_2\text{L}(\mu\text{-PhPO}_4)(\text{NO}_3)]^+$ complex cations; (b) and (c) detailed views of an asymmetrical half unit of the complex. Two close water molecules in each complex cation involved in $\text{HOH}\cdots\text{OPO}_3^{2-}$ hydrogen bonds are also represented.

In addition to the above mentioned coordination features, in each complex cation two water-mediated hydrogen bonds are found, established between two secondary amines of the macrocycle and an uncoordinated oxygen atom of the dianion ($\text{O4A}\cdots\text{O16w}\cdots\text{N1A}$ with distances of 2.649(8) and 2.916(8) Å and $\text{O4A}\cdots\text{O15w}\cdots\text{N28A}$ with distances of 2.782(9) and 3.317(10) Å, $\text{O4B}\cdots\text{O17w}\cdots\text{N28B}$ with distances of 2.622(8) and 2.994(8) Å and $\text{O4B}\cdots\text{O11w}\cdots\text{N1B}$ with distances of 2.574(8) and 2.932(8) Å), see Table S5 in the ESI. Twenty other water molecules and three

nitrate anions are found in the crystal structure but are not directly involved in the binding event (see Fig. S4 in the ESI).

Bearing in mind that the chemistry of phenylphosphate is very rich especially with Cu, a Cambridge Structural Database (CSD) survey was carried out to analyze the data retrieved for complexes in which phosphate behaves either as monodentate or bidentate $\mu_2\text{-}\eta^1\text{:}\eta^1$ or $\mu\text{-}\eta^1$ bridging ligand in copper(II) complexes. This survey showed that in 40% of the cases the phosphate moiety plays a monodentate role, in other 40% the phosphate works as a bridge between two Cu through coordination of two oxygen atoms ($\mu_2\text{-}\eta^1\text{:}\eta^1$), and only in 20% of the cases the phosphate acts as a bridge using only one O atom ($\mu\text{-}\eta^1$). Furthermore, all the bonds distances and angles reported for the structure disclosed herein are in agreement with the data reported at CSD.

Table 3 Selected bond distances (Å) and angles (°) in the coordination spheres of the $[\text{Cu}_2\text{L}(\mu\text{-PhPO}_4)]^{2+}$ (A) and $[\text{Cu}_2\text{L}(\mu\text{-PhPO}_4)(\text{NO}_3)]^+$ (B) cation complexes

Complex	A	B
Distances / Å		
N1–Cu1	2.068(6)	2.072(7)
N10–Cu1	2.092(8)	2.077(5)
N8–Cu1	1.925(6)	1.921(6)
O1–Cu1	1.872(4)	1.875(6)
O1C–Cu2	–	2.393(8)
N19–Cu2	2.083(6)	2.084(6)
N26–Cu2	1.929(6)	1.924(6)
N28–Cu2	2.073(6)	2.063(6)
O3–Cu2	1.862(6)	1.859(6)
Cu1...Cu2	5.812(1)	5.811(1)
Angles / °		
N1–Cu1–N10	164.4(2)	162.3(2)
N8–Cu1–O1	171.5(2)	164.6(3)
O1C–Cu2–N19	–	94.1(3)
O1C–Cu2–N28	–	90.1(3)
O1C–Cu2–N26	–	86.2(3)
O1C–Cu2–O3	–	100.9(3)
N19–Cu2–N28	160.9(2)	162.1(2)
N26–Cu2–O3	173.5(2)	173.6(3)

Computational Studies. In spite of our efforts, it was not possible to obtain crystals of the $[\text{Cu}_2\text{L}(\mu\text{-OH})]^{3+}$ complex suitable for X-ray diffraction studies. To overcome this problem, the structure of this hydroxocomplex was investigated by using DFT calculations in aqueous solution (see computational

details below). The minimum energy conformation obtained from these calculations presents a conformation of the ligand with the ethyl groups at position 3 of each of the phenyl rings pointing to the same side of the ligand. This is in contrast to the structure observed in the solid state for $[\text{Cu}_2\text{L}(\mu\text{-PhPO}_4)(\text{NO}_3)]^+$, in which these ethyl groups are pointing to opposite sides with respect to the macrocycle main plane. This conformation of the ligand brings the two copper centres at a distance of only 3.94 Å (5.81 Å for $[\text{Cu}_2\text{L}(\mu\text{-PhPO}_4)(\text{NO}_3)]^+$ in the solid state) aided by the presence of a bridging hydroxide anion that provides a $\text{Cu}\cdots\text{O}\cdots\text{Cu}$ angle of 167.3° . Each copper centre presents a distorted square planar coordination geometry composed of three nitrogen donors from the 2,6-bis(aminomethyl)pyridine moieties of the macrocycle and one oxygen atom of the bridging anion, see Fig. 4.

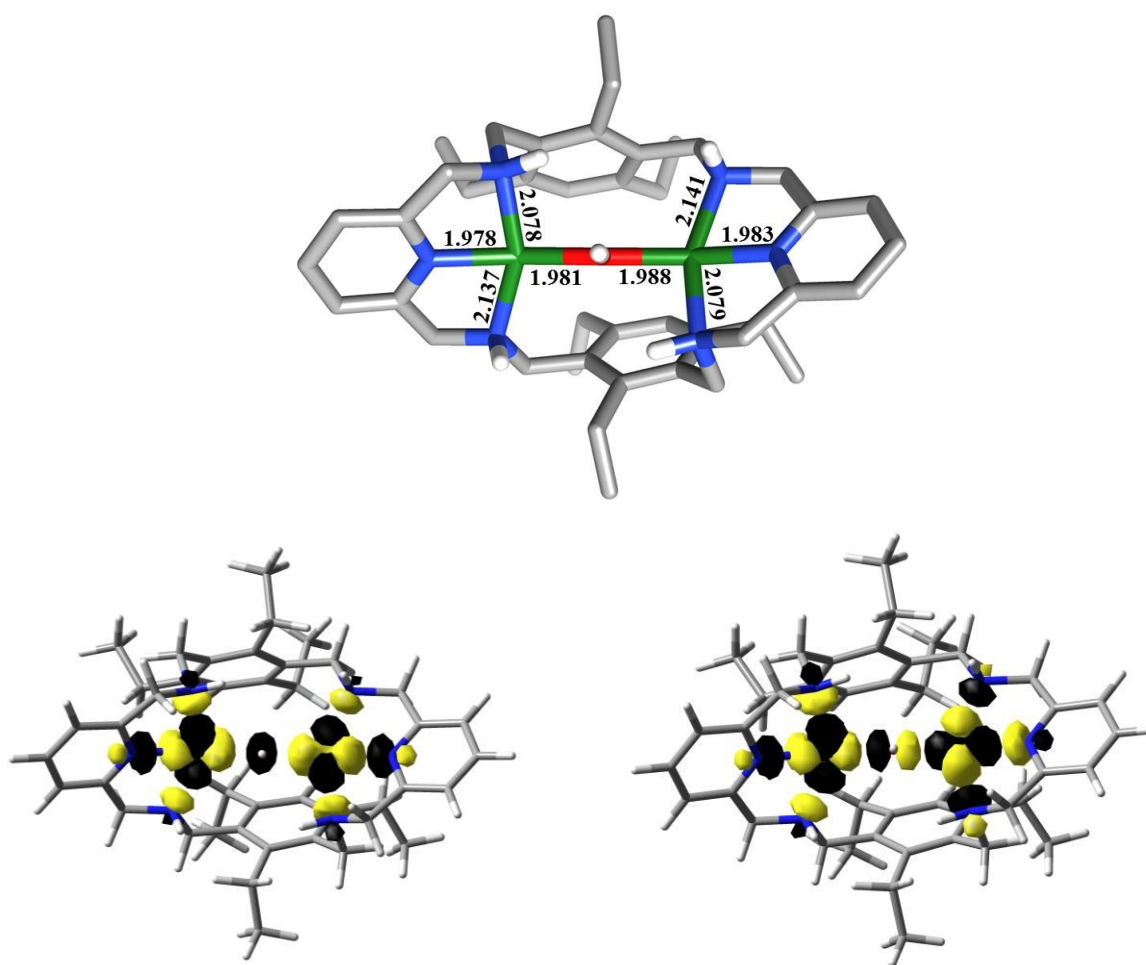


Fig. 4 Top: Structure of $[\text{Cu}_2\text{L}(\mu\text{-OH})]^{3+}$ obtained with DFT calculations (M06/TZVP, bulk solvent effects considered using a polarized continuum) and bond distances of the metal coordination environments (Å). Bottom: Active magnetic orbitals of $[\text{Cu}_2\text{L}(\mu\text{-OH})]^{3+}$ obtained with CASSCF(2,2) calculations.

The Cu...Cu distance in $[\text{Cu}_2\text{L}(\mu\text{-OH})]^{3+}$ is of the order of that found in the two dinuclear copper(II) $\mu\text{-OH}$ complexes of macrocyclic ligands,²⁰ and practically identical to the $\mu\text{-hydroxo-dicopper(II)}$ polyazacryptate²¹ already studied. In the former structures involving macrocyclic ligands the Cu...Cu distance are 3.284 Å^{20a} and 3.642 Å,^{20b} and the copper(II) centres are in approximate square-planar geometry. However, the Cu...O...Cu angles of around 132°^{20a} and 143°^{20b}, respectively, are considerably smaller. Only one structure of a dinuclear copper(II) complex with polyazacryptand is available in the literature.²⁴ In this $\mu\text{-hydroxo-dicopper(II)}$ cryptate the copper centres were found to have trigonal-bipyramidal geometry, with a Cu...Cu separation of 3.9 Å and an almost linear Cu–OH–Cu motif (174.0°). Additionally, an effective antiferromagnetic interaction $J_{iso} = 865 \text{ cm}^{-1}$ was found ($J_{iso}\mathbf{S}_1\cdot\mathbf{S}_2$, $J_{iso} > 0$ indicates antiferromagnetic interaction), due to the collinear disposition of bridge O 2p_z and copper(II) magnetic orbitals that makes this hydroxo-bridged derivative diamagnetic.²⁴

Complete active space self-consistent field (CASSCF) calculations were conducted to assess the relative energies of the triplet and singlet states of $[\text{Cu}_2\text{L}(\mu\text{-OH})]^{3+}$. Our CASSCF calculations considered the minimal active space (CASSCF(2,2)), where the two unpaired electrons occupy the two magnetic orbitals.²⁵ Inspection of the magnetically active orbitals (Fig. 4) shows that they correspond to the symmetric and antisymmetric combinations of the Cu 3d_{x²-y²} orbitals with tails on the bridging hydroxide ligand and the nitrogen atoms of the macrocycle. At the CASSCF(2,2) level the $[\text{Cu}_2\text{L}(\mu\text{-OH})]^{3+}$ complex presents antiferromagnetic coupling, as the singlet state is the ground state, with the triplet state having an energy of 39.7 cm⁻¹ with respect to the former. The inclusion of dynamic correlation using the NEVPT2 method (see computational details below) increases this energy difference to 66.1 cm⁻¹. These results are in qualitative agreement with the EPR studies described below.

The isotropic coupling constant characterizing the magnetic interaction in $[\text{Cu}_2\text{L}(\mu\text{-OH})]^{3+}$ was further investigated using the DFT studies with the broken-symmetry approach. We found that B3LYP/6-311G(d) calculations provide a calculated exchange coupling constant ($J_{iso} = 898 \text{ cm}^{-1}$) in excellent agreement with the experimental value ($J_{iso} = 865 \pm 50 \text{ cm}^{-1}$)^{24b} for the cryptate reported by Nelson (Table S6 in the ESI).²⁴ The same computational approach gives an isotropic coupling constant of $J_{iso} = 443 \text{ cm}^{-1}$ ($J_{iso}\mathbf{S}_1\cdot\mathbf{S}_2$, $J_{iso} > 0$ means anti-ferromagnetic coupling) for $[\text{Cu}_2\text{L}(\mu\text{-OH})]^{3+}$.

EPR Studies

In an effort to gain insight into the structures of the dinuclear copper(II) complexes and the corresponding phosphonate cascade complexes in solution, EPR spectroscopic measurements were

carried out in H₂O:MeOH (50:50 v/v) frozen solutions at 110–135 K. Spectra of the dinuclear copper complexes of L were recorded at two different pH values, and the cascade complexes of PhPO₄²⁻ and HpST1²⁻ at the pH corresponding to the maximum percentage of the cascade species, which is of ~ 6.0 (see Fig. S3 in the ESI).

Several of the X-band EPR spectra collected are typical of dinuclear copper(II) complexes, corresponding to the triplet state of a coupled dinuclear copper site with a total spin $S = 1$, see Figs. 5 and 6. Two different types of signals are observed: intense signals at around 3000 G ($g \sim 2$) corresponding to $\Delta M_s = \pm 1$ transitions; and weak signals at ca. 1600 G ($g \sim 4$ region) from the $\Delta M_s = 2$ transition.²⁶ In our case, only at certain conditions, very faint and lacking hyperfine splitting signals were detected at the latter region (not shown). In some of our spectra (traces C in Figs. 5 and 6b), the signal at $g \sim 2$ presents a well-resolved seven-line hyperfine pattern due to the interaction of both copper nuclei (nuclear spin $I_{\text{Cu}} = 3/2$, $2I_{\text{Cu}} + 1 = 7$).²⁶

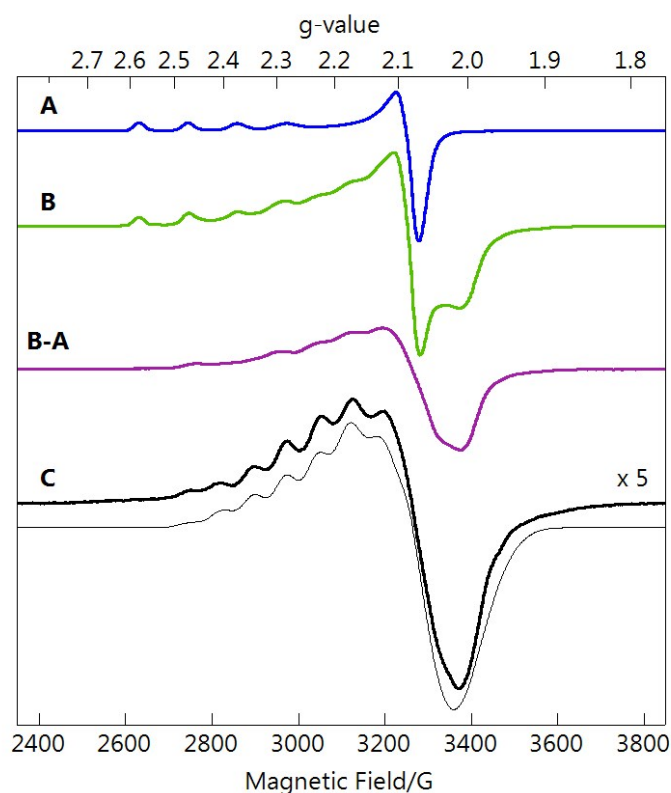


Fig. 5 X-band EPR spectra of (A) 1.94 mM Cu(NO₃)₂, (B) Cu²⁺:L (2:1) at pH 4.5 with C_L = 5.04 mM, (B-A) is the spectrum that results after subtracting spectrum A to spectrum B, and (C) Cu²⁺:L (2:1) at pH 7.0 with C_L = 4.39 mM (the signal intensity is multiplied by 5). The thinner line is a computer simulation with spin Hamiltonian parameters mentioned in the text. All spectra recorded at 135 K, 2.0 mW microwave power, 1.0 mT modulation amplitude, and frequency (ν) of 9.5 GHz. All samples in H₂O:MeOH (50:50 v/v) solution.

Trace B in Fig. 5 is the EPR spectrum of the $\text{Cu}^{2+}:\text{L}$ solution (2:1 ratio) at pH 4.5, and consists of several species. The features in the range 2630–2970 G and the peak at 3280 G indicate the presence of *ca.* 19% of $\text{Cu}(\text{NO}_3)_2$ (represented by trace A). Trace B-A is spectrum B after subtracting the contribution of $\text{Cu}(\text{NO}_3)_2$, and reveals an EPR spectrum that suggests mono- and dinuclear copper(II) complexes, in agreement with the species distribution diagram in Fig. 1b. Trace C represents the EPR spectrum for a $\text{Cu}^{2+}:\text{L}$ (2:1) solution at pH 7.0. Under these conditions only the $[\text{Cu}_2\text{L}(\mu\text{-OH})]^{3+}$ complex is expected to exist in solution (Fig. 1b). Due to its large isotropic coupling constant of $J_{iso} = 443 \text{ cm}^{-1}$ ($J_{iso}\mathbf{S}_1\cdot\mathbf{S}_2$, $J_{iso} > 0$ indicates anti-ferromagnetic coupling) obtained from DFT calculations and expected for these type of complexes,²⁷ this hydroxo-bridged species is essentially diamagnetic because the ground state is $S = 0$ and the triplet state at X-band EPR conditions is not thermally accessible and thus EPR silent, i.e. one should obtain no signal.^{24,27} Therefore, the EPR signal in trace C from Fig. 5 corresponds to an unknown species denoted by **1**. This species may be attributed to a non-bridged hydroxo complex, which cannot be distinguished from the bridged species using potentiometry, but the formation of other species under the conditions used for EPR measurements (*i.e.* dinuclear species containing nitrate or water ligands) cannot be ruled out. The EPR spectrum of species **1** could be simulated²⁸ assuming $J_{iso} = 2.0 \text{ cm}^{-1}$ (so that the triplet state is thermally accessible) and the parameters listed in Table 4. According to these simulations species **1** represents about 46% of all possible dicopper species present in solution. Therefore, about 54 % of all possible dicopper species in solution are EPR silent. Since the hydroxo-bridged species should be EPR silent one can infer that 54 % corresponds to $[\text{Cu}_2\text{L}(\mu\text{-OH})]^{3+}$. The relatively long $\text{Cu}\cdots\text{Cu}$ distance obtained for species **1** from EPR spectral simulation (6.63(2) Å, Table 4) points to binuclear species lacking bridging ligands. Additional evidence that the EPR signal tends to vanish at higher pH is provided by the evolution of the EPR spectra of $\text{Cu}^{2+}:\text{L}$ (2:1) with pH (Fig. S5 in the ESI).

In the Fig. 6a is shown the X-band EPR spectrum of the cascade dicopper(II) complex of L with PhPO_4^{2-} obtained at pH 5.8 and 110 K. The thinner trace is a computer simulation²⁸ using the parameters given in Table 4 for $[\text{Cu}_2\text{L}(\mu\text{-PhPO}_4)]^{2+}$, which represents about 95 % of all possible dicopper complexes present in solution. Although the crystal structure shows two complexes with different coordination environments at one of the copper sites, the EPR spectra suggest that in frozen solution only one species is present. It is also worthwhile to note that the values for J_{iso} and $\text{Cu}\cdots\text{Cu}$ distance obtained from the EPR simulation (-17 cm^{-1} and 5.45 Å, Table 4) are very similar to the ones obtained from DFT calculations (B3LYP/6-311G(d)) for both structures: -18.7 cm^{-1} and 5.56 Å for $[\text{Cu}_2\text{L}(\mu\text{-PhPO}_4)]^{2+}$ and -16.8 cm^{-1} and 5.66 Å for $[\text{Cu}_2\text{L}(\mu\text{-PhPO}_4)(\text{NO}_3)]^+$. Thus, the analysis of the

EPR data provide solid evidence for the formation of dinuclear copper(II) species containing a PhPO_4^{2-} anion bridging both metals.

Table 4 X-band EPR spectroscopic data for the copper(II) complexes in solution determined by computer simulation.²⁸

Parameter	Species 1	$[\text{Cu}_2\text{L}(\mu\text{-PhPO}_4)]^{2+}$	$[\text{Cu}_2\text{L}(\mu\text{-HpST1})]^{2+}$
$g_{x_1} = g_{x_2}$	2.02(5)	2.08(2)	2.06(2)
$g_{y_2} = g_{y_2}$	2.09(4)	2.08(5)	2.08(5)
$g_{z_2} = g_{z_2}$	2.25(3)	2.24(3)	2.27(3)
$A_{x_1} = A_{x_2}^a$	38(2)	48(2)	45(2)
$A_{y_1} = A_{y_2}^a$	39(2)	43(2)	41(2)
$A_{z_1} = A_{z_2}^a$	156(4)	155(4)	165(4)
$J_{iso} \text{ (cm}^{-1}\text{)}$	2.0	-17(1)	-16(1)
$\text{Cu}\cdots\text{Cu} \text{ (\AA)}$	6.63(2)	5.45(2)	5.94(6)
$\theta \text{ (}^\circ\text{)}^b$	~ 42	~ 34	~ 35

^a Values of A in 10^{-4} cm^{-1} . ^b θ is the angle between the inter-copper coupling vector and the g_z directions.

The cascade species formed in solution upon addition of HpST1^{2-} at pH 5.6 provide an EPR spectrum at 127 K that can be simulated²⁸ assuming the formation of three species (Fig. 6b): species **1** (trace **A**, 0.25 mM), $\text{Cu}(\text{NO}_3)_2$ (trace **B**, 0.62 mM) and $[\text{Cu}_2\text{L}(\mu\text{-HpST1})]^{2+}$ (trace **C**, 1.44 mM). Therefore, *ca.* 85% of the binuclear copper(II) species correspond to the cascade complex of HpST1^{2-} with a bridging phosphate moiety and the rest can be assigned to species **1**. The similarity of all parameters obtained from EPR simulated spectra for both cascade complexes support the idea that in both cases the PhPO_4^{2-} group is well accommodated between the Cu sites.

The simulated EPR spectrum of the cascade complex species formed with PhPO_4^{2-} indicates a $\text{Cu}\cdots\text{Cu}$ separation of 5.45 Å, which is close to the 5.81 Å found in the corresponding structure determined by X-ray diffraction pointing to a very similar structure in solution with PhPO_4^{2-} anion bridging the two copper centres. The spectra with the studied peptides are both very similar and also similar to the one with PhPO_4^{2-} (see Fig. 6a and Table 4), pointing also to similar structures in solution.

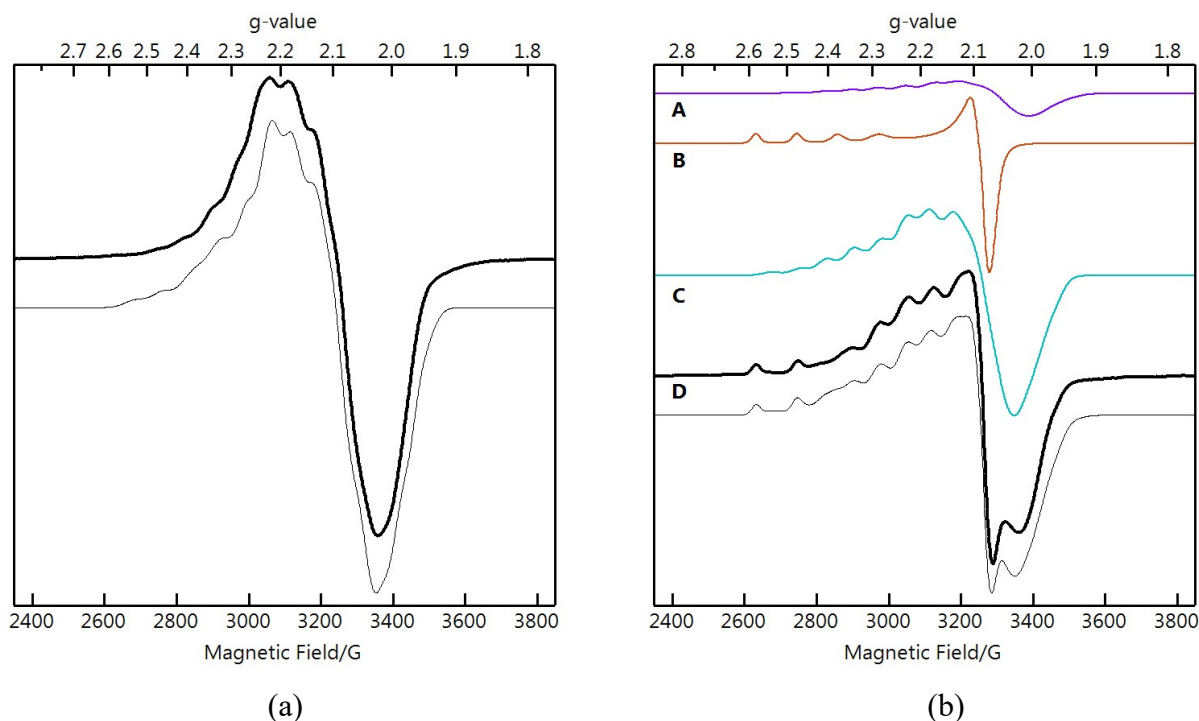


Fig. 6 X-band EPR spectra for: (a) solution of the dicopper(II) cascade complex of L with PhPO_4^{2-} at pH 5.8 and 110 K for $\text{Cu}^{2+}:\text{L}$ (2:1) with $C_L = 2.0$ mM, and PhPO_4^{2-} concentration of 4 mM. The thinner line is obtained by computer simulation using parameters in Table 4 for $[\text{Cu}_2\text{L}(\mu\text{-PhPO}_4)]^{2+}$ and corresponds to *ca.* 1.9 mM. (b) Thicker trace D corresponds to the cascade complex solution with HpST1^{2-} at pH 5.6 and 127 K for $\text{Cu}^{2+}:\text{L}$ (2:1) (2.0 mM) with $C_L = 2.0$ mM. The thinner trace D is the sum of three species represented by traces A to C obtained by computer simulation with parameters on Table 4. Trace A represents 0.25 mM of **1**, trace B represents 0.62 mM of $\text{Cu}(\text{NO}_3)_2$ and 1.44 mM of $[\text{Cu}_2\text{L}(\mu\text{-HpST1})]^{2+}$ corresponds to trace C. All spectra recorded at 2.0 mW microwave power, 1.0 mT modulation amplitude, and frequency (ν) of 9.5 GHz. All samples in $\text{H}_2\text{O}:\text{MeOH}$ (50:50 v/v) solution.

CONCLUSIONS

A new triethylbenzene-derived tetraazamacrocyclic containing pyridyl spacers was prepared in good yield by a “one-pot” procedure. The corresponding dinuclear copper(II) complexes were studied as receptors for the recognition of phosphorylated peptides in aqueous solution.

Single-crystal X-ray diffraction determination of the dicopper(II) complex of L showed the copper centres at a distance of 5.81 Å from one another, with the phosphate group of the PhPO_4^{2-} substrate well accommodated between them. A similar structure for this cascade complex, and for the other cascade complexes with all the phosphorylated anions studied, is found in solution by EPR studies.

DFT studies of the $[\text{Cu}_2\text{L}(\mu\text{-OH})]^{3+}$ complex revealed a conformation of the ligand that brings the two copper centres at a very short distance of 3.94 Å aided by the presence of a bridging hydroxide anion that provides a $\text{Cu}\cdots\text{O}\cdots\text{Cu}$ angle of 167.3°. This complex is diamagnetic, as proved by EPR

experiments and CASSCF calculations, and it coexists in solution with a complex in a different conformation, in lower percentage, with a Cu...Cu distance of 6.63 Å.

It was found that the receptor forms very stable associations with the several protonated forms of the phosphorylated peptides, with constant values ranging 3.96–5.35 log units, with the affinity of the receptor towards the H₃pST1 peptide being slightly higher than towards the H₂pST3 one, in water:methanol 50:50 v/v. These promising results suggest the potential use of this complex as a binder of phosphorylated STAT proteins upon slight modifications of the ligand in order to become it soluble in water. Such studies will be described in due course.

EXPERIMENTAL SECTION

General considerations. All solvents and reagents used were purchased from commercial sources, had reagent grade quality and were used as supplied without further purification, except 2,6-pyridinedicarbaldehyde, which was prepared according to literature methods.²⁹ The H₂pST3 peptide was obtained commercially through CASLO ApS (mass spectrometry certificates can be found in Fig. S6, and NMR spectra made by us in Figs. S7–S8 in the ESI).¹⁰ All NMR spectra were recorded on a Bruker Avance III 400 (¹H at 400.13 MHz and ¹³C at 100.61 MHz). TMS was used as a reference for the ¹H NMR measurements in CDCl₃. Peak assignments were based in peak integration and multiplicity for 1D ¹H spectra, and 2D COSY, NOESY, HMQC and HMBC experiments. Microanalyses were carried out by the ITQB Microanalytical Service. Mass spectra have been acquired in the positive mode, after direct injection of the sample solutions with a syringe pump into a Bruker Daltonics Esquire 3000plus mass spectrometer equipped with an ESI source.

Caution! Although no problems were encountered during this work with the organic and inorganic azides, these compounds should be considered potentially explosive.

Syntheses

Synthesis of the peptide H₃pST1. The H₃pST1 peptide (Scheme 1) was synthesized by using Fmoc chemistry.¹⁸ The peptide was assembled on a rink amide MBHA (4-methylbenzhydrylamine) resin using the HBTU–HOBt–DIEA [N,N,N',N'-tetramethyl-O-(1H-benzotriazol-1-yl)uronium hexafluorophosphate (1-hydroxybenzotriazole) – N,N-diisopropylethylamine] activation method and was acetylated in the N-terminal using 10% acetic anhydride in DMF. Cleavage and removal of the protecting groups were simultaneously performed by treatment with a mixture of TFA–TIS–water (95:2.5:2.5 % v/v) for 2 h at r.t. and under nitrogen. The solution was filtered to remove the resin and then evaporated under a nitrogen stream. Cold diethyl ether was added to precipitate the crude peptide which was purified by preparative reversed-phase HPLC in a Phenomenex Jupiter Proteo column

(250×21.20 mm, 4 μm, 90 Å) using solvent A (99.9% H₂O–0.1% TFA) and solvent B (90% CH₃CN–9.9% H₂O–0.1% TFA) mixtures. H₃pST1 was eluted from the column with a linear gradient from 0 to 25 % B in 12 min at a flow rate of 10 mL min⁻¹ (*R_t* = 18 min). The purity of the peptide was checked by analytical reversed-phase HPLC (Phenomenex Jupiter Proteo column, 250×4.6 mm, 4 μm, 90 Å) and it was higher than 95%. The peptide H₃pST1 was obtained as a white fluffy solid (0.200 g) with a yield of 19%. ¹H NMR (400 MHz, D₂O) δ 0.81–0.87 (6 H, m, 2×CH₃ Ile), 1.12–1.20 (1 H, m, γ-CHH Ile), 1.19 (3 H, d, *J* = 6.9 Hz, CH₃ Thr), 1.29–1.48 (5 H, m, 2×CH₂ Lys + γ-CHH Ile), 1.73–1.82 (3 H, m, CH₂ Lys + β-CH Ile), 1.89–1.95 (1 H, m, β-CHH Glu), 1.93 (3 H, s, CH₃CO), 2.03–2.08 (1 H, m, β-CHH Glu), 2.21–2.26 (2 H, m, γ-CH₂ Glu), 2.57 (2 H, t, *J* = 6.7 Hz, ε-CH₂ Lys), 2.85–3.07 (2 H, m, β-CH₂ Tyr), 4.13–4.20 (2 H, m, β-CH Thr + α-H Glu), 4.24–4.28 (2 H, m, α-H Thr + α-H Ile), 4.33–4.37 (1 H, m, α-H Lys), 4.51–4.55 (1 H, m, α-H Tyr), 7.13 (4 H, q, *J* = 8.7 Hz, 4×H-bz) ppm. ¹³C NMR (101 MHz, D₂O) δ 9.81 (CH₃ Ile), 14.67 (CH₃ Ile), 18.74 (γ-CH₂ Ile), 18.82 (CH₃ Thr), 21.52 (CH₃CO), 22.39 (CH₂ Lys), 30.74 (CH₂ Lys), 31.32 (CH₂ Lys), 33.60 (γ-CH₂ Glu), 34.00 (β-CH₂ Glu), 35.98 (β-CH Ile), 36.18 (β-CH₂ Tyr), 40.29 (ε-CH₂ Lys), 53.53 (α-C Ile), 53.82 (α-C Lys), 55.14 (α-C Tyr), 55.26 (α-C Glu), 57.89 (α-C Thr), 66.92 (β-CH Thr), 120.40 (C3/C5-bz), 129.74 (C2/C6-bz), 130.04 (C1-bz), 153.02 (C4-bz), 170.94 (CH₃CO), 171.81 (C=O Ile), 173.06 (C=O Tyr), 173.33 (C=O Thr), 174.03 (C=O Glu), 181.37 (C=O Lys), 182.08 (CO₂H Glu) ppm. ESI-MS (MeOH) *m/z* 398.6 [M + H + Na]²⁺; 774.2 [M + H]⁺; 796.1 [M + Na]⁺, see Figs. S9–S13 in the ESI.

Syntheses of L and intermediate compounds

2,4-bis(bromomethyl)-1,3,5-triethylbenzene.³⁰ To a solution of 1,3,5-triethylbenzene (9.41 mL, 0.05 mol), paraformaldehyde (4.50 g, 0.15 mol) and glacial acetic acid (25 mL) were added 3 equiv. of HBr/AcOH 33% (26 mL) under stirring. The solution was stirred at 80 °C under nitrogen for 8 h. Afterwards, the solution was poured into distilled water (50 mL) and the precipitate formed was filtered off. The solid residue was transferred to a separation funnel with water (50 mL) and extracted with CHCl₃ (3×40 mL). The organic layer was dried with anhydrous Na₂SO₄, filtered and evaporated to dryness. The product was purified by column chromatography in silica gel using n-hexane as eluent to give a white powder. Yield: 13.4 g, 77%. ¹H NMR (400 MHz, CDCl₃) δ (ppm): 1.28–1.36 (9 H, m, CH₃ C_{1,5}-ethyl and C₃-ethyl), 2.77 (4 H, q, *J* = 7.5 Hz, CH₂ C_{1,5}-ethyl), 2.94 (2 H, q, *J* = 7.7 Hz, CH₂ C₃-ethyl), 4.61 (4 H, s, CH₂Br), 6.98 (1 H, s, H6 bz), see Fig. S14 in the ESI.

2,4-bis(azidomethyl)-1,3,5-triethylbenzene. To a solution of 2,4-bis(bromomethyl)-1,3,5-triethylbenzene (4.25 g, 12.2 mmol) in DMF (125 mL) were added small portions of NaN₃ (3.17 g, 48.8 mmol) during 30 min under stirring. The solution was stirred under nitrogen for 24 h. The NaBr that precipitated was filtered through Celite and the solution was evaporated to dryness. The residue

was dissolved in CH_2Cl_2 (100 mL), transferred to a separation funnel and washed with water (2×100 mL) and with a NaCl saturated solution (100 mL). The organic layer was dried with anhydrous Na_2SO_4 , filtered and evaporated to dryness to give an orange oil. Yield: 3.14 g, 94%. ^1H NMR (400 MHz, CDCl_3) δ (ppm): 1.21–1.29 (9 H, m, CH_3 $\text{C}_{1,5}$ -ethyl and C_3 -ethyl), 2.74 (4 H, q, $J = 7.4$ Hz, CH_2 $\text{C}_{1,5}$ -ethyl), 2.84 (2 H, q, $J = 7.7$ Hz, CH_2 C_3 -ethyl), 4.46 (4 H, s, CH_2N_3), 7.05 (1 H, s, H6 bz). ^{13}C NMR (100 MHz, CDCl_3) δ (ppm): 15.66 (CH_3 $\text{C}_{1,5}$ -ethyl), 16.12 (CH_3 C_3 -ethyl), 22.87 (CH_2 C_3 -ethyl), 26.47 (CH_2 $\text{C}_{1,5}$ -ethyl), 47.77 (CH_2N_3), 127.77 (C6), 128.78 (C2 and C4), 143.89 (C3), 144.78 (C1 and C5), see Figs. S15–S20 in the ESI.

2,4-bis(aminomethyl)-1,3,5-triethylbenzene. To a round bottom flask with 2,4-bis(azidomethyl)-1,3,5-triethylbenzene (3.14 g, 11.5 mmol) were added small portions of triphenylphosphine (12.11 g, 46.2 mmol) followed by a 10:1 THF/ H_2O solution (29 mL). The mixture was stirred under nitrogen for 24 h and then it was evaporated to dryness. The residue was dissolved in CH_2Cl_2 (20 mL), transferred to a separating funnel and washed with a 1 M HCl solution (3×20 mL). The aqueous phases were combined, extracted with ethyl acetate (4×25 mL) and 3 M NaOH was added until pH 12. After that, the aqueous phase was extracted with CHCl_3 (3×40 mL). The organic layer was dried with anhydrous Na_2SO_4 , filtered and evaporated to dryness to give an orange oil. Yield: 1.84 g, 73%. ^1H NMR (400 MHz, CDCl_3) δ (ppm): 1.21–1.27 (9 H, m, CH_3 $\text{C}_{4,6}$ -ethyl and C_2 -ethyl), 2.71 (4 H, q, $J = 7.4$ Hz, CH_2 $\text{C}_{4,6}$ -ethyl), 2.85 (2 H, q, $J = 7.7$ Hz, CH_2 C_2 -ethyl), 3.87 (4 H, s, CH_2NH_2), 6.95 (1 H, s, H5 bz). ^{13}C NMR (100 MHz, CDCl_3) δ (ppm): 16.27 (CH_3 $\text{C}_{4,6}$ -ethyl), 17.11 (CH_3 C_2 -ethyl), 22.49 (CH_2 C_2 -ethyl), 26.12 (CH_2 $\text{C}_{4,6}$ -ethyl), 39.49 (CH_2NH_2), 127.71 (C5), 136.78 (C1 and C3), 141.01 (C2), 141.68 (C4 and C6), see Figs. S21–26 in the ESI.

L. To a solution of 2,4-bis(aminomethyl)-1,3,5-triethylbenzene (0.80 g, 3.7 mmol) in CH_2Cl_2 (71 mL) and MeOH (35 mL) was added 2,6-pyridinedicarboxaldehyde (0.50 g, 3.7 mmol) under stirring. The solution was left overnight with stirring and under nitrogen. The solution was evaporated to dryness at r.t. and MeCN was added (60 mL). The precipitate formed was isolated by filtration and washed with MeCN (2×40 mL) (0.89 g, 77%). ^1H NMR (400 MHz, CDCl_3) δ (ppm): 1.18–1.22 (18 H, m, CH_3 $\text{C}_{4,6}$ -ethyl and C_2 -ethyl), 2.30 (4 H, q, $J = 7.0$ Hz, CH_2 C_2 -ethyl), 2.50 (8 H, m, CH_2 $\text{C}_{4,6}$ -ethyl), 5.09 (8 H, s, bz- CH_2N), 7.05 (2 H, s, H5 bz), 7.77 (2 H, t, $J = 7.85$ Hz, H4 pyr), 7.83 (4 H, s, pyr-CHN), 8.12 (4 H, d, $J = 7.83$ Hz, H3 and H5 pyr), see Fig. S27 in the ESI. The precipitate (0.89 g, 1.4 mmol) was then dissolved in MeOH (80 mL) and solid NaBH_4 (0.42 g, 11.1 mmol) was added in small portions to avoid excessive foaming. Upon this addition, the mixture was left under stirring at r.t. until the bubbling ceased, and then refluxed for 4 h. The solution was filtered and evaporated under vacuum almost to dryness, then water was added (20 mL) and the remaining MeOH was evaporated. Afterwards, the

solution was made strongly basic with 6 M KOH and extracted with CHCl_3 (3×50 mL). The organic layer was dried with anhydrous Na_2SO_4 , filtered and evaporated to give a white powder. Yield: 0.83 g (70%). ^1H NMR (400 MHz, CDCl_3) δ (ppm): 1.05 (6 H, t, $J = 7.52$ Hz, CH_3 C_2 -ethyl), 1.23 (12 H, t, $J = 7.45$ Hz, CH_3 $\text{C}_{4,6}$ -ethyl), 1.88 (4 H, s, NH), 2.72–2.83 (12 H, m, CH_2 $\text{C}_{4,6}$ -ethyl and C_2 -ethyl), 3.72 (8 H, s, bz- CH_2N), 3.97 (8 H, s, pyr- CH_2N), 6.92 (2 H, s, H5 bz), 7.12 (4 H, d, $J = 7.30$ Hz, H3 and H5 pyr), 7.58 (2 H, t, $J = 7.73$ Hz, H4 pyr). ^{13}C NMR (100MHz, CDCl_3) δ (ppm): 15.99 (CH_3 $\text{C}_{4,6}$ -ethyl), 17.45 (CH_3 C_2 -ethyl), 22.45 (CH_2 C_2 -ethyl), 26.19 (CH_2 $\text{C}_{4,6}$ -ethyl), 46.78 (bz- CH_2N), 55.74 (pyr- CH_2N), 121.03 (C3 and C5 pyr), 127.28 (C5 bz), 133.49 (C1 and C3 bz), 136.76 (C4 pyr), 142.07 (C2 pyr), 142.86 (C4 and C6 bz), 159.34 (C2 and C4 pyr). Elem. Anal. found: C, 73.00; H, 8.17; N, 12.33. Calc. for $\text{C}_{42}\text{H}_{58}\text{N}_6 \cdot 0.4\text{CHCl}_3$: C, 73.31; H, 8.17; N, 12.10%; ESI-MS (MeOH) m/z 647.5 $[\text{M} + \text{H}]^+$, see Figs. S28–S34 in the ESI.

Synthesis of dicopper(II) complexes. The ligand L (2.0 mmol) and the $\text{Cu}(\text{NO}_3)_2$ (4 mmol), from standard titrated solutions, were dissolved in MeOH:H₂O (50:50, 10.0 mL) and 0.10 M KOH was added to adjust the pH value to 6.5. The solution was stirred overnight. ESI-MS (H₂O/MeOH, pH = 6.5) m/z 913.3 $[\text{Cu}_2\text{L}(\text{OH})(\text{NO}_3)_2]^+$; 385.2 $[\text{Cu}_2\text{L}-2\text{H}]^{2+}$ (see Fig. S35 in the ESI). The UV-vis of the complex at pH 7.0 is shown at Fig. S37 (left) in the ESI.

Synthesis of $[\text{Cu}_2\text{L}(\mu\text{-PhPO}_4)][\text{Cu}_2\text{L}(\mu\text{-PhPO}_4)(\text{NO}_3)]3\text{NO}_3 \cdot 24\text{H}_2\text{O}$. The ligand L (3.3 mg, 4 μmol) was dissolved in MeOH:H₂O (50:50, 4 mL) and 0.002 M $\text{Cu}(\text{NO}_3)_2$ (8 μmol), and 0.001 M phenylphosphoric acid (4 μmol) solutions were added. The pH was adjusted to 5.1 with KOH solution. The solution was allowed to slowly evaporate at r.t. Dark blue single crystals suitable for X-ray crystallographic determination were obtained within 7 days. ESI-MS (MeOH) m/z 472.1 $[\text{Cu}_2\text{L}(\text{PhPO}_4)]^{2+}$; 385.2 $[\text{Cu}_2\text{L}-2\text{H}]^{2+}$ (see Fig. S36 in the ESI). The UV-vis of this cascade complex at pH 5.8 and $\text{Cu}^{2+}:\text{L}:\text{HPhPO}_4^-$ 2:1:1 ratio is shown at Fig. S37 (right) in the ESI.

Potentiometric measurements. Reagents and solutions. All the solutions were prepared in a H₂O/MeOH (50:50 v/v) mixed solvent. A stock solution of L was prepared at *ca.* 2.0×10^{-3} M with 0.0225 M HNO_3 maintaining the 50:50 proportion of water/methanol. Phosphate and phenyl phosphate solutions were prepared from the corresponding acids. A stock solution of $\text{Cu}(\text{NO}_3)_2$ (analytical grade) was prepared at about 2.5×10^{-2} M and the exact concentrations checked by titration with $\text{K}_2\text{H}_2\text{edta}$ following standard methods.³¹ Carbonate-free solutions of the KOH titrant were prepared from a Merck ampoule diluted to 500 mL of water (freshly boiled for about 2 h and allowed to cool under nitrogen) to which 500 mL of MeOH were added. These solutions were discarded every time carbonate concentration was about 0.5% of the total amount of base. The titrant solutions were standardized by Gran's method.³²

Equipment and working conditions. The equipment used was described before.^{10,33} A Metrohm 6.0123.100 glass electrode and a Metrohm 6.0733.100 Ag/AgCl reference electrode were used for the measurements. The ionic strength of the experimental solutions was kept at 0.10 ± 0.01 M with KNO_3 , the temperature was maintained at 298.2 ± 0.1 K. Atmospheric CO_2 was excluded from the titration cell during experiments by passing purified nitrogen across the top of the experimental solution.

Measurements. The $[\text{H}^+]$ of the solutions was determined by the measurement of the electromotive force of the cell, $E = E^{\circ} + Q \times \log [\text{H}^+] + E_j$. The term pH is defined as $-\log [\text{H}^+]$. E° , Q , E_j and K_w were determined by titration of a solution of known hydrogen-ion concentration at the same ionic strength, using the acid pH range of the titration. The liquid-junction potential, E_j , was found to be negligible under the experimental conditions used. The value of K_w was determined from data obtained in the alkaline range of the titration, considering E° and Q valid for the entire pH range and found to be equal to $10^{-13.86}$ in our experimental conditions. Before and after each set of titrations the glass electrode was calibrated as a $[\text{H}^+]$ probe by titration of a 1.000×10^{-3} M standard HNO_3 solution with standard KOH. Every measurement was carried out with 0.040 mmol of ligand L in a total volume of 40.00 mL, except for the measurements involving peptides ($\text{H}_2\text{pST3}$ and $\text{H}_3\text{pST1}$), where 0.010 mmol of the peptide in a total volume of 15.00 mL was used. The exact concentration of L and of the peptidic substrates was obtained by titration with a standard KOH solution. Copper(II) complexation experiments were performed in the presence of $\text{Cu}(\text{NO}_3)_2$ in 1:1 and 2:1 $C_{\text{Cu}}:C_{\text{L}}$ ratios. The ternary systems measurements were carried out in the simultaneous presence of L, $\text{Cu}(\text{NO}_3)_2$ and each anion at 2:1:1 M:L:S ratios (L = ligand, M = metal and S = substrate). In each titration 85 to 120 points were collected, and a minimum of two titration curves were performed. All the substrates were independently titrated alone and in the presence of copper(II) ion at 0.5:1, 1:1 and 2:1 $C_{\text{Cu}}/C_{\text{S}}$ ratios and the respective equilibrium constants used in the calculations. Backtitrations with standard HNO_3 solution were performed to confirm the values of the final E° readings.

Calculation of equilibrium constants. Overall protonation constants, β_i^{H} , of the free ligand L and of the studied substrates, the overall stability constants of complexes, $\beta_{\text{M}_m\text{H}_h\text{L}_l}$ and the overall association constants of the complexes of L with the substrates, $\beta_{\text{M}_m\text{H}_h\text{L}_l\text{S}_s}$, were calculated by fitting the potentiometric data obtained for all the performed titrations in the same experimental conditions with the Hyperquad program.³⁴ The hydrolysis constants for copper(II) were held constant during data refinement. The initial computations were obtained in the form of overall constants, $\beta_{\text{H}_h\text{L}} = [\text{H}_h\text{L}_l]/[\text{H}]^h[\text{L}]^l$, $\beta_{\text{M}_m\text{H}_h\text{L}_l} = [\text{M}_m\text{H}_h\text{L}_l]/[\text{M}]^m[\text{H}]^h[\text{L}]^l$ or $\beta_{\text{M}_m\text{H}_h\text{L}_l\text{S}_s} = [\text{M}_m\text{H}_h\text{L}_l\text{S}_s]/[\text{M}]^m[\text{H}]^h[\text{L}]^l[\text{S}]^s$. The errors quoted are the standard deviations of the overall constants given directly by the program for the

input data, which include all the experimental points of all titration curves. The errors quoted for the stepwise constant values were calculated using the propagation rules. The HySS program³⁵ was used to calculate the concentration of equilibrium species from the calculated constants from which distribution diagrams were plotted. The species considered in a particular model were those that could be justified by the principles of coordination and supramolecular chemistry.

EPR Spectroscopy. The X-band EPR spectra were recorded in perpendicular-mode with a Bruker EMX 8/2.7 spectrometer equipped with continuous-flow cryostat for liquid nitrogen. EPR spectra simulations and species concentrations were determined with the software SpinCount developed by M. P. Hendrich.²⁸ EPR signals were quantified by relative to a 5 mM Cu(NO₃)₂ in H₂O:MeOH (50:50 v/v) solution. The spin Hamiltonian used for computer simulations is as follows,

$$H = \beta\mathbf{B}\cdot\mathbf{g}_1\cdot\mathbf{S}_1 + \beta\mathbf{B}\cdot\mathbf{g}_2\cdot\mathbf{S}_2 + \mathbf{S}_1\cdot\mathbf{A}_1\cdot\mathbf{I}_1 + \mathbf{S}_2\cdot\mathbf{A}_2\cdot\mathbf{I}_2 + \mathbf{S}_1\cdot\mathbf{J}\cdot\mathbf{S}_2$$

where 1 and 2 denote the two copper ions ($S_1 = S_2 = 1/2$). The first two terms represent the electronic Zeeman interactions, and the third and fourth terms the hyperfine interactions. The term $\mathbf{S}_1\cdot\mathbf{J}\cdot\mathbf{S}_2$ contains both the isotropic (exchange, $J_{iso}\mathbf{S}_1\cdot\mathbf{S}_2$, $J_{iso} > 0$ means anti-ferromagnetic coupling) and anisotropic (dipolar) spin-spin interactions. This term, is calculated from values of J_{iso} , the inter-copper distances (Cu...Cu), and the angles describing the relative orientations of the two \mathbf{g} tensors and the inter-copper vector.^{36,37}

EPR samples were prepared in H₂O/MeOH (50:50 v/v) using stock solutions of L (8.9×10^{-3} M), Cu(NO₃)₂ (5.0×10^{-2} M), H₂PhPO₄ (5.0×10^{-2} M) and H₃pST1 (2.3×10^{-3} M). The copper(II) complexes and cascade complex solutions were prepared from the stock solutions at the different pH by addition of standard KOH solutions (0.1 and 0.01 M). Sample concentrations are mentioned in the text.

Single Crystal X-ray Diffraction. Crystals of [Cu₂L(μ-PhPO₄)] [Cu₂L(μ-PhPO₄)(NO₃)] 3NO₃·24H₂O suitable for X-ray diffraction study were mounted with Fomblin© in a cryoloop. Data were collected on a Bruker AXS-KAPPA APEX II diffractometer with graphite-monochromated radiation (MoKα, $\lambda = 0.71073$ Å) at 150 K. The X-ray generator was operated at 50 kV and 30 mA and the X-ray data collection was monitored by the APEX2³⁸ program. All data were corrected for Lorentzian, polarization and absorption effects using the SAINT³⁸ and SADABS³⁸ programs. SIR97³⁹ and SHELXS-97⁴⁰ were used for structure solution and SHELXL-97⁴⁰ for full matrix least-squares refinement on F^2 . These three programs are included in the package of programs WINGX-Version 2014.1.⁴¹ The crystals quality and their diffraction were very poor. Even though many crystals were tested, the presented data set are the best data possible for these crystals. The low ratio of observed reflections is due to very weak crystals. Yet, the anisotropic refinement was possible. Non-hydrogen atoms were refined anisotropically. A full-matrix least-squares refinement was used for the non-

hydrogen atoms with anisotropic thermal parameters. All the hydrogen atoms were inserted in idealized positions and allowed to refine in the parent carbon atom. There is one disordered nitrate in the structure, for which a model was determined (to better represent this model, coordinates do not form a properly connected set - alert B at checkcif). Hydrogen atoms of water molecules have not been added as they were not possible to locate from the electron density map. Furthermore, some water molecules are disordered but it was not possible to accurately model that disorder, what is reflected in the checkcif generating alerts B regarding short distances between atoms.

Molecular diagrams presented are drawn with PyMOL.⁴² PLATON⁴³ was used to calculate bond distances and angles as well as hydrogen bond interactions. In Table 6 the data collection and refinement details are summarized. CCDC 1499385 contains the supplementary crystallographic data for this article.

Table 6 Crystallographic data and structure refinement details for [Cu₂L(μ-PhPO₄)]₂[Cu₂L(μ-PhPO₄)(NO₃)]₂·3NO₃·24H₂O

chemical formula	C ₉₆ H ₁₂₆ O ₄₄ Cu ₄ N ₁₆ P ₂
formula weight	2524.22
temperature, K	150(2)
wavelength, Å	0.71073
crystal form, colour	Block, blue
crystal size, mm	0.17×0.07×0.03
crystal system	Triclinic
space group	P-1
<i>a</i> , Å	12.6536(6)
<i>b</i> , Å	18.7909(9)
<i>c</i> , Å	26.3285(12)
α (°)	81.480(2)
β (°)	79.723(2)
γ (°)	88.933(2)
<i>V</i> , Å ³	6091.8(5)
<i>Z</i>	2
<i>F</i> (000)	2624
<i>d</i> (mg.cm ⁻³)	1.376
μ (mm ⁻¹)	0.803
θ range (°)	1.941 – 25.242
reflections collected/unique	24795/11252
<i>R</i> _{int}	0.1095
GoF	1.048
Final <i>R</i> indices [<i>I</i> > 2σ(<i>I</i>)]	<i>R</i> ₁ = 0.0926, ^a <i>wR</i> ₂ = 0.2086 ^b

$$^a R_1 = \sum ||F_o| - |F_c|| / \sum |F_o|. \quad ^b wR_2 = [\sum [w(F_o^2 - F_c^2)^2] / \sum [w(F_o^2)^2]]^{1/2}$$

Computational methods. Full geometry optimizations of the $[\text{Cu}_2\text{L}(\text{OH})]^{3+}$ and $[\text{Cu}_2\text{L}(\mu\text{-PhPO}_4)]^{2+}$ complexes were performed in aqueous solution employing DFT calculations within the hybrid meta-GGA approximation with the M06 exchange-correlation functional⁴⁴ and the Gaussian 09 package (Revision D.01).⁴⁵ In these calculations we used the standard Ahlrichs' split valence (SVP)⁴⁶ and triple- ξ (TZVP)⁴⁷ basis sets including polarization functions. Both basis sets provide very similar optimized structures. Solvent effects (water) were included by using the polarizable continuum model (PCM). In particular we employed the integral equation formalism (IEFPCM) variant as implemented in Gaussian 09.⁴⁸ No symmetry constraints have been imposed during the optimizations. The nature of the optimized geometries as true energy minima was confirmed by using frequency analysis (0 imaginary frequencies). The default values for the integration grid (75 radial shells and 302 angular points) and the SCF energy convergence criteria (10^{-8}) were used in all calculations.

Nonrelativistic energy levels and wave functions were computed using the Complete Active Space Self-Consistent Field (CASSCF) method⁴⁹ and the ORCA program package (Version 3.0.3)⁵⁰ along with the TZVP basis set. CASSCF calculations were performed by using an active space including two electrons distributed into the two magnetically active Cu 3d-based molecular orbitals (CASSCF(2,2)). The RIJCOSX approximation⁵¹ was used to speed up the calculations using the Def2-TZVPP/J auxiliary basis set as constructed automatically by ORCA. The CASSCF wavefunctions were subsequently analyzed using N-electron valence perturbation theory to second order (NEVPT2).⁵² Solvent effects (water) were taken into account by using the conductor-like screening model (COSMO)⁵³ as implemented in ORCA.

DFT calculations were employed to estimate isotropic exchange coupling constants using the broken-symmetry approach originally introduced by Noodleman.⁵⁴ Since the value for the exchange coupling constants for the various complexes studied have a wide range, it is advised to use a modification of Noodleman's approach that was carry out by Yamaguchi and co-workers,⁵⁵ who obtained

$$J_{iso} = 2 (E_{SCF(HS)} - E_{SCF(BS)}) / (\langle S^2 \rangle_{HS} - \langle S^2 \rangle_{BS})$$

where $\langle S^2 \rangle_{HS}$, $\langle S^2 \rangle_{BS}$ and $E_{SCF(HS)}$, $E_{SCF(BS)}$ are expectation values of the spin-squared operator determinants and the energies for the HS and BS, respectively. The Yamaguchi expression is valid for the whole range of coupling strengths and reduces to the Noodleman equation in the weak coupling limit.⁵⁴ In these calculations we tested Becke's three parameter hybrid functional (B3LYP) besides the M06 functional, in combination with either TZVP or 6-311G(d) basis sets. Both ORCA and Gaussian were used for BS calculations, providing virtually identical results. Since the B3LYP/6-311G(d) method provided the best results for the reference compound reported by Nelson,^{24b} subsequent

calculations employed this method to estimate the coupling constants of $[\text{Cu}_2\text{L}(\mu\text{-OH})]^{3+}$, $[\text{Cu}_2\text{L}(\mu\text{-PhPO}_4)]^{2+}$ and $[\text{Cu}_2\text{L}(\mu\text{-PhPO}_4)(\text{NO}_3)]^+$, see Tables S7–S11 in the ESI. The ferromagnetic (HS, for High Spin) and broken-symmetry (BS) optimizations were carried out by utilizing the Gaussian 09 built-in “fragments” module, and an initial guess wavefunction was generated and used as a starting point for the optimization calculations. The geometry optimizations were terminated upon reaching the default convergence criteria. The optimizations did not impose any symmetry. The frequencies for the equilibrium conformation obtained with the FREQ keyword were all positive, indicating the identification of a minimum.

Conflict of interest

The authors declare no competing financial interest.

ACKNOWLEDGEMENTS

The authors acknowledge Fundação para a Ciência e a Tecnologia (FCT) for the financial support and the fellowships of L. Mesquita and of R. Fernandes under Project PTDC/QEQ-SUP/2718/2012. The authors also acknowledge support by FCT under Project PTDC/BIA-PRO/101837/2008, and under project RECI/BBB-BQB/0230/2012 for the NMR spectrometers as part of the National NMR Facility. The X-ray facilities thank FCT for funding (RECI/QEQ-QIN/0189/2012). M. C. Almeida from the ITQB Analytical Services Unit is acknowledged for providing elemental analysis and ESI-MS data. P. Mateus and V. André acknowledge FCT for the fellowships SFRH/BPD/79518/2011 and SFRH/BPD/78854/2011, respectively. C. P.-I. thanks Centro de Supercomputación de Galicia for providing the computer facilities.

REFERENCES

- 1 G. Manning, D. B. Whyte, R. Martinez, T. Hunter and S. Sudarsanam, *Science*, 2002, **298**, 1912–1934.
- 2 a) H. Patterson, R. Nibbs, I. McInnes and S. Siebert, *Clin. Exp. Immunol.*, 2013, **176**, 1–10; b) M. J. Jembrek, M. Babić, N. Pivac, P. R. Hof and G. Šimić, *Transl. Neurosci.*, 2013, **4**, 466–476.
- 3 J. Brognard and T. Hunter, *Curr. Opin. Genet. Dev.*, 2011, **21**, 4–11.
- 4 J. A. Ubersax and J. E. Ferrell Jr, *Nat. Rev. Mol. Cell Biol.*, 2007, **8**, 530–541.
- 5 a) A. Ojida, Y. Miyahara, T. Kohira and I. Hamachi, *Biopolymers*, 2004, **76**, 177–184; b) A. Ojida and I. Hamachi, *Bull. Chem. Soc. Jpn.*, 2006, **79**, 35–46; c) H. T. Ngo, X. Liu and K. A. Jolliffe,

- Chem. Soc. Rev.* 2012, **41**, 4928–4965; d) R. Kubota and I. Hamachi, *Chem. Soc. Rev.*, 2015, **44**, 4454–4471.
- 6 A. E. Hargrove, S. Nieto, T. Zhang, J. L. Sessler and E. V. Anslyn, *Chem. Rev.*, 2011, **111**, 6603–6782.
- 7 a) A. Ojida, Y. Mito-oka, M.-a. Inoue and I. Hamachi, *J. Am. Chem. Soc.*, 2002, **124**, 6256–6258; b) A. Ojida, Y. Mito-oka, M.-a. Inoue and I. Hamachi, *J. Am. Chem. Soc.* 2003, **125**, 10184–10185; c) A. Ojida, Y. Mito-oka, K. Sada and I. Hamachi, *J. Am. Chem. Soc.*, 2004, **126**, 2454–2463; d) A. Ojida, M.-a. Inoue, Y. Mito-oka, H. Tsutsumi, K. Sada and I. Hamachi, *J. Am. Chem. Soc.*, 2006, **128**, 2052–2058; e) A. Grauer, A. Riechers, S. Ritter and B. König, *Chem. Eur. J.*, 2008, **14**, 8922–8927; f) T. Sakamoto, M.-a. Inoue, A. Ojida and I. Hamachi, *Bioorg. Med. Chem. Lett.*, 2009, **19**, 4175–4177; g) Y. Ishida, M.-a. Inoue, T. Inoue, A. Ojida and I. Hamachi, *Chem. Commun.*, 2009, 2848–2850; h) A. Ojida, T. Sakamoto, M.-a. Inoue, S.-h. Fujishima, G. Lippens and I. Hamachi, *J. Am. Chem. Soc.*, **2009**, *131*, 6543–6548; i) J. A. Drewry, S. Fletcher, P. Yue, D. Marushchak, W. Zhao, S. Sharmeen, X. Zhang, A. D. Schimmer, C. Gradinaru, J. Turkson and P. T. Gunning, *Chem. Commun.*, **2010**, *46*, 892–894; j) A. Riechers, A. Grauer, S. Ritter, B. Sperl, T. Berg and B. König, *J. Mol. Recognit.*, **2010**, *23*, 329–334; k) H. Akiba, J. Sumaoka and M. Komiyama, *Chem. Eur. J.*, **2010**, *16*, 5018–5025; l) M. Bhuyan, E. Katayev, S. Stadlbauer, H. Nonaka, A. Ojida, I. Hamachi and B. König, *Eur. J. Org. Chem.*, **2011**, 2807–2817; m) S. Zhang, L. Han, C. Li, J. Wang, W. Wang, Z. Yuan and X. Gao, *Tetrahedron*, **2012**, *68*, 2357–2362; n) J. A. Drewry, E. Duodu, A. Mazouchi, P. Spagnuolo, S. Burger, C. C. Gradinaru, P. Ayers, A. D. Schimmer and P. T. Gunning, *Inorg. Chem.*, **2012**, *51*, 8284–8291; o) J. H. Kang, H. J. Kim, T.-H. Kwon and J.-I. Hong, *J. Org. Chem.*, **2014**, *79*, 6000–6005; p) H. Akiba, J. Sumaoka, T. Hamakubo and M. Komiyama, *Anal. Bioanal. Chem.*, **2014**, *406*, 2957–2964; q) D. Kraskouskaya, M. Bancercz, H. S. Soor, J. E. Gardiner and P. T. Gunning, *J. Am. Chem. Soc.*, **2014**, *136*, 1234–1237.
- 8 P. Mateus, L. M. P. Lima and R. Delgado, *Polyhedron*, 2013, **52**, 25–42.
- 9 a) R. J. Motekaitis and A. E. Martell, *Inorg. Chem.*, 1992, **31**, 5534–5542; b) R. J. Motekaitis and A. E. Martell, *Inorg. Chem.*, 1994, **33**, 1032–1037; c) P. E. Jurek, A. E. Martell, R. J. Motekaitis and R. D. Hancock, *Inorg. Chem.*, 1995, **34**, 1823–1829; d) Q. Lu, J. J. Reibenspies, A. E. Martell and R. J. Motekaitis, *Inorg. Chem.*, 1996, **35**, 2630–2636; e) D. A. Nation, A. E. Martell, R. I. Carroll and A. Clearfield, *Inorg. Chem.*, 1996, **35**, 7246–7252; f) J. B. English, A. E. Martell, R. J. Motekaitis and I. Murase, *Inorg. Chim. Acta*, 1997, **258**, 183–192; g) D. A. Nation, Q. Lu and A. E. Martell, *Inorg. Chim. Acta*, 1997, **263**, 209–217; h) Q. Lu, J. H. Reibenspies, R. I. Carroll, A. E. Martell and A. Clearfield, *Inorg. Chim. Acta*, 1998, **270**, 207–215; i) T. F. Pauwels, W. Lippens, G. G. Herman and

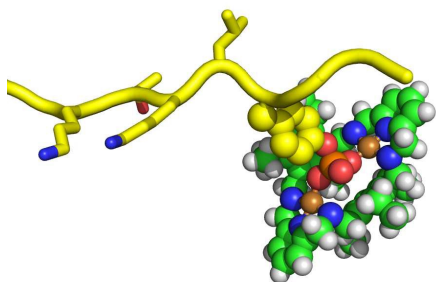
- A. M. Goeminne, *Polyhedron*, 1998, **17**, 1715–1723; j) A. E. Martell, R. J. Motekaitis, Q. Lu and D. A. Nation, *Polyhedron*, 1999, **18**, 3203–3218; k) L. Fabbrizzi, N. Marcotte, F. Stomeo and A. Taglietti, *Angew. Chem., Int. Ed.*, 2002, **41**, 3811–3814; l) N. Marcotte and A. Taglietti, *Supramol. Chem.*, 2003, **15**, 617–625; m) J. E. Barker, Y. Liu, N. D. Martin and T. Ren, *J. Am. Chem. Soc.*, 2003, **125**, 13332–13333; n) M. A. Saeed, D. R. Powell and M. A. Hossain, *Tetrahedron Lett.*, 2010, **51**, 4904–4907; o) V. Amendola, G. Bergamaschi, A. Buttafava, L. Fabbrizzi and E. Monzani, *J. Am. Chem. Soc.*, 2010, **132**, 147–156.
- 10 (a) H. Akiba, J. Sumaoka, and M. Komiyama, *Chem. Eur. J.*, 2010, **16**, 5018–5025; b) J. Sumaoka, H. Akiba, and M. Komiyama, *Int. J. Anal. Chem.*, vol. 2016, Article ID 3216523, 14 pages. doi:10.1155/2016/3216523; c) L. M. Mesquita, F. Herrera, C. V. Esteves, P. Lamosa, V. André, P. Mateus and R. Delgado, *Inorg. Chem.*, 2016, **55**, 3589–3598.
- 11 X. Chen, U. Vinkemeier, Ya. Zhao, D. Jeruzalmi, J. E. Darnell Jr. and J. Kuriyan, *Cell*, 1998, **93**, 827–839.
- 12 S. Becker, B. Groner and C. W. Müller, *Nature*, 1998, **394**, 145–151.
- 13 J. E. Darnell Jr., *Science*, 1997, **277**, 1630–1635.
- 14 L. A. Cabell, M. D. Best, J. J. Lavigne, S. E. Schneider, D. M. Perreault, M.-K. Monahan and E. V. Anslyn, *J. Chem. Soc., Perkin Trans. 2*, 2001, 315–323.
- 15 A. W. van der Made and R. H. van der Made, *J. Org. Chem.*, 1993, **58**, 1262–1263.
- 16 K. J. Wallace, R. Hanes, E. V. Anslyn, J. Morey, K. V. Kilway and J. Siegel, *Synthesis*, 2005, 2080–2083.
- 17 P. Mateus, R. Delgado, P. Brandão and V. Félix, *J. Org. Chem.*, 2009, **74**, 8638–8646.
- 18 *Fmoc Solid Phase Peptide Synthesis: A Practical Approach*, Eds.: W. C. Chan, P. D. White, Oxford University Press, New York, 2000.
- 19 P. Mateus, R. Delgado, F. Lloret, J. Cano, P. Brandão and V. Félix, *Chem. Eur. J.*, 2011, **17**, 11193–11203.
- 20 a) R. J. Motekaitis, A. E. Martell, J.-M. Lehn and E.-I. Watanabe, *Inorg. Chem.*, 1982, **21**, 4253–4251; b) R. Menif, J. Reibenspies and A. E. Martell, *Inorg. Chem.*, 1991, **30**, 3446–3454; c) F. Arnaud-Neu, S. Fuangwasdi, B. Maubert, J. Nelson and V. McKee, *Inorg. Chem.*, 2000, **39**, 573–579.
- 21 a) P. L. Burk, J. A. Osborn, M.-T. Youinou, Y. Agnus, R. Louis and R. Weiss, *J. Am. Chem. Soc.*, 1981, **103**, 1273–1274; b) P. K. Coughlin and S. J. Lippard, *J. Am. Chem. Soc.*, 1981, **103**, 3228–3231.
- 22 I. Sóvágó, C. Kállay and K. Várnagy, *Coord. Chem. Rev.*, 2012, **256**, 2225–2233.

- 23 A. W. Addison, T. N. Rao, J. Reedijk, J. van Rijn and G. C. Verschoor, *J. Chem. Soc., Dalton Trans.*, 1984, 1349–1356.
- 24 a) C. J. Harding, V. McKee, J. Nelson and Q. Lu, *J. Chem. Soc., Chem. Commun.*, 1993, 1768–1770. b) Q. Lu, J.-M. Latour, C. J. Harding, N. Martin, D. J. Marrs, V. McKee and J. Nelson, *J. Chem. Soc., Dalton Trans.*, 1994, 1471–1478.
- 25 R. P. Sharma, A. Saini, P. Venugopalan, V. Ferretti, F. Spizzo, C. Angeli and C. J. Calzado, *New J. Chem.*, 2014, **38**, 574–583.
- 26 T. D. Smith and J. R. Pilbrow, *Coord. Chem. Rev.*, 1974, **13**, 173–278.
- 27 D. L. Reger, A. E. Pascui, E. A. Foley, M. D. Smith, J. Jezierska and A. Ozarowski, *Inorg. Chem.*, 2014, **53**, 1975–1988.
- 28 D. Petasis and M. Hendrich, *Quantitative Interpretation of Multifrequency Multimode EPR Spectra of Metal Containing Proteins*, *Method Enzymol*, 2015, **563**, 171–208. The authors thank Prof. Hendrich for the special support on the simulation of the epr spectra presented.
- 29 N. W. Alcock, R. G. Kingston, P. Moore and C. Pierpoint, *J. Chem. Soc., Dalton Trans.*, 1984, 1937–1943.
- 30 A. Metzger, V. M. Lynch and E. V. Anslyn, *Angew. Chem., Int. Ed.*, 1997, **36**, 862–865.
- 31 G. Schwarzenbach and W. Flaschka, *Complexometric Titrations*, Methuen & Co, London, 1969, 252–258.
- 32 F. J. Rossotti and H. J. Rossotti, *J. Chem. Educ.*, 1965, **42**, 375–378.
- 33 C. V. Esteves, J. Madureira, L. M. P. Lima, P. Mateus, I. Bento and R. Delgado, *Inorg. Chem.*, 2014, **53**, 4371–4386.
- 34 P. Gans, A. Sabatini and A. Vacca, *Talanta*, 1996, **43**, 1739–1753.
- 35 L. Alderighi, P. Gans, A. Ienco, D. Peters, A. Sabatini and A. Vacca, *Coord. Chem. Rev.*, 1999, **184**, 311–318.
- 36 A. Bencini and D. Gatteschi, *Electron Paramagnetic Resonance of Exchange Coupled Systems*. Springer: 1990.
- 37 B. Bennett, W. E. Antholine, V. M. D'souza, G. Chen, L. Ustinyuk and R. C. Holz, *J. Am. Chem. Soc.*, 2002, **124**, 13025–13034.
- 38 Bruker Saints and Bruker SADABS, *Bruker Analytical Systems: Madison*, W. I., 2005.
- 39 A. Altomare, M. C. Burla, M. Camalli, G. L. Cascarano, C. Giacovazzo, A. Guagliardi, A. G. G. Moliterni, G. Polidori and R. Spagna, *J. Appl. Cryst.*, 1999, **32**, 115–119.
- 40 G. M. Sheldrick, *Acta Crystallogr. A*, 2008, **64**, 112–122.
- 41 L. J. Farrugia, *J. Appl. Cryst.*, **1999**, **32**, 837–838.

- 42 The PyMOL Molecular Graphics System, Version 1.2r3pre, Schrödinger, LLC.
- 43 A. L. Spek, PLATON, *Acta Crystallogr. D*, 2009, **65**, 148–155.
- 44 Y. Zhao and D. G. Truhlar, *Theor. Chem. Acc.*, 2008, **120**, 215–241.
- 45 Gaussian 09, Revision D.01, M. J. Frisch, G. W. Trucks, H. B. Schlegel, G. E. Scuseria, M. A. Robb, J. R. Cheeseman, G. Scalmani, V. Barone, B. Mennucci, G. A. Petersson, H. Nakatsuji, M. Caricato, X. Li, H. P. Hratchian, A. F. Izmaylov, J. Bloino, G. Zheng, J. L. Sonnenberg, M. Hada, M. Ehara, K. Toyota, R. Fukuda, J. Hasegawa, M. Ishida, T. Nakajima, Y. Honda, O. Kitao, H. Nakai, T. Vreven, J. A. Montgomery Jr., J. E. Peralta, F. Ogliaro, M. Bearpark, J. J. Heyd, E. Brothers, K. N. Kudin, V. N. Staroverov, R. Kobayashi, J. Normand, K. Raghavachari, A. Rendell, J. C. Burant, S. S. Iyengar, J. Tomasi, M. Cossi, N. Rega, N. J. Millam, M. Klene, J. E. Knox, J. B. Cross, V. Bakken, C. Adamo, J. Jaramillo, R. Gomperts, R. E. Stratmann, O. Yazyev, A. J. Austin, R. Cammi, C. Pomelli, J. W. Ochterski, R. L. Martin, K. Morokuma, V. G. Zakrzewski, G. A. Voth, P. Salvador, J. J. Dannenberg, S. Dapprich, A. D. Daniels, Ö. Farkas, J. B. Foresman, J. V. Ortiz, J. Cioslowski and D. J. Fox, Gaussian, Inc., Wallingford CT, 2009.
- 46 A Schaefer, H. Horn and R. Ahlrichs, *J. Chem. Phys.*, 1992, **97**, 2571–2577.
- 47 A. Schaefer, C. Huber and R. Ahlrichs, *J. Chem. Phys.*, 1994, **100**, 5829–5835.
- 48 J. Tomasi, B. Mennucci and R. Cammi, *Chem. Rev.*, 2005, **105**, 2999–3093.
- 49 P.-A. Malqvist and B. O. Roos, *Chem. Phys. Lett.*, 1989, **155**, 189–194.
- 50 F. Neese, The ORCA Program System. *Wiley Interdiscip. Rev.: Comput. Mol. Sci.*, 2012, **2**, 73–78.
- 51 a) F. Neese, F. Wennmohs, A. Hansen and U. Becker, *Chem. Phys.*, 2009, **356**, 98–109; b) R. Izsak and F. Neese, *J. Chem. Phys.*, 2011, **135**, 144105; c) T. Petrenko, S. Kossmann and F. Neese, *J. Chem. Phys.*, 2011, **134**, 054116; d) S. Kossmann and F. Neese, *Chem. Phys. Lett.*, 2009, **481**, 240–243.
- 52 a) C. Angeli, R. Cimiraglia and J.-P. Malrieu, *Chem. Phys. Lett.*, 2001, **350**, 297–305; b) C. Angeli, R. Cimiraglia and J.-P. Malrieu, *J. Chem. Phys.*, 2002, **117**, 9138–9153; c) C. Angeli, R. Cimiraglia, S. Evangelisti, T. Leininger and J.-P. Malrieu, *J. Chem. Phys.*, 2001, **114**, 10252–10264; d) C. Angeli and R. Cimiraglia, *Theor. Chem. Acc.*, 2002, **107**, 313–317.
- 53 S. Sinnecker, A. Rajendran, A. Klamt, M. Diedenhofen and F. Neese, *J. Phys. Chem. A*, 2006, **110**, 2235–2245.
- 54 L. Noodleman, *J. Chem. Phys.*, 1981, **74**, 5737–5743.
- 55 T. Soda, Y. Kitagawa, T. Onishi, Y. Takano, Y. Shigeta, H. Nagao, Y. Yoshioka and K. Yamaguchi, *Chem. Phys. Lett.*, 2000, **319**, 223–230.

Recognition of Phosphopeptides by a Dinuclear Copper(II) Macrocyclic Complex in Water:Methanol 50:50 v/v solution

L. M. Mesquita, P. Mateus, R. D. V. Fernandes, O. Iranzo, V. André, F. Tiago de Oliveira, C. Platas-Iglesias, R. Delgado*



The dinuclear copper(II) complex of a triethylbenzene-derived hexaazamacrocyclic was able to recognize phosphorylated substrates in water:methanol (50:50 v/v) solution.